J|A|C|S
ARTICLES
Published on Web 01/21/2006

Electroreduction of a Series of Alkylcobalamins: Mechanism of Stepwise Reductive Cleavage of the Co−C Bond

Ronald L. Birke,* Qingdong Huang, Tudor Spataru, and David K. Gosser, Jr.

Contribution from the Department of Chemistry and Center for Analysis of Structures and Interfaces (CASI), The City College of New York, and The Graduate School and University Center of The City University of New York, New York, New York 10031

Received July 6, 2005; E-mail: birke@sci.ccny.cuny.edu

Abstract: The electrochemical (EC) reduction mechanism of methylcobalamin (Me-Cbl) in a mixed DMF/MeOH solvent in 0.2 M tetrabutylammonium fluoroborate electrolyte was studied as a function of temperature and solvent ratio vs a nonaqueous Ag/AgCl/Cl^- reference electrode. Double-potential-step chronoamperometry allowed the rate constant of the subsequent homogeneous reaction to be measured over the temperature range from 0 to −80 °C in 40:60 and 50:50 DMF:MeOH ratios. Activation enthalpies are 5.8 ± 0.5 and 7.6 ± 0.3 kcal/mol in the 40:60 and 50:50 mixtures of DMF/MeOH, respectively. Digital simulation and curve-fitting for an EC mechanism using a predetermined homogeneous rate constant of 5.5×10^3 s^{-1} give $E^{\circ\prime} = -1.466$ V, $k^\circ = 0.016$ cm/s, and $\alpha = 0.77$ at 20 °C for a quasi-reversible electrode process. Digital simulation of the results of Lexa and Savéant (*J. Am. Chem. Soc.* **1978**, *100*, 3220−3222) shows that the mechanism is a series of stepwise homogeneous equilibrium processes with an irreversible step following the initial electron transfer (ET) and allows estimation of the equilibrium and rate constants of these reactions. An electron coupling matrix element of $\bar{H}_{kA} = (4.7 \pm 1.1) \times 10^{-4}$ eV (~46 J/mol) is calculated for the nonadiabatic ET step for reduction to the radical anion. A reversible bond dissociation enthalpy for homolytic cleavage of Me-Cbl is calculated as 31 ± 2 kcal/mol. The voltammetry of the ethyl-, *n*-propyl-, *n*-butyl-, isobutyl-, and adenosyl-substituted cobalamin was studied, and estimated reversible redox potentials were correlated with Co−C bond distances as determined by DFT (B3LYP/ LANL2DZ) calculations.

Introduction

Alkylcorrinoids function as cofactors in a number of mammalian and prokaryotic enzyme systems, the most well studied being the cobalamin (Cbl)-dependent enzymes with cofactors of methylcobalamin (Me-Cbl) and adenosylcobalamin (Ado-Cbl), the so-called coenzymes of vitamin B_{12}. These cofactors contain a cobalt−carbon bond which is cleaved during the enzymatic reaction. The organometallic bond in Me-Cbl is a σ bond between the cobalt ion and a methyl carbon of the axial methyl ligand, whereas in Ado-Cbl it is a σ bond between the cobalt ion and the 5′ carbon of the 5′-deoxy-5′-adenosyl axial ligand. In methylcobalamin-dependent enzymes, which catalyze methyl transfer, the Co−C bond appears to be cleaved heterolytically to form vitamin B_{12s}, called cob(I)alamin or $Cbl(I)^-$, whereas in adenosylcobalamin-dependent enzymes, which catalyze group migrations, the Co−C bond appears to be cleaved homolytically to form vitamin B_{12r}, called cob(II)alamin or Cbl(II). Although much research has focused on the mechanism of activation of Co−C bond cleavage in vitamin B_{12} compounds and coenzyme enzymatic systems, the molecular details which explain why this bond-breaking process is so different in the two classes of vitamin B_{12}-dependent enzymatic systems and how the bond is activated for cleavage still have not been resolved.

In this article we focus on the Co−C bond cleavage of alkylcobalamins that are germane to the vitamin B_{12}-dependent methyl transferase enzymes. An important step in methyl transferase reactions is the transfer of a methyl group from Me-Cbl to a substrate, such as to homocysteine (Hcy) in the methionine synthase reaction. The rate of this reaction is enhanced by a factor of 2.5×10^9 for enzyme-bound Hcy and Me-Cbl compared to the reaction rate of the unbound species and by about 10^3 for bound Me-Cbl compared to exogenous Me-Cbl when Hcy is enzyme bound.[1] The study of structural, electronic configuration, and solvent factors which affect the cleavage rate for various alkylcobalamins in solution should be relevant to the biochemical reactions of alkylcobalamins (R-Cbl). Herein, we further investigate the electrochemical (EC) reductive cleavage mechanism of R-Cbl (R-B_{12}) by varying the alkyl group R in a dimethylformamide/methanol solvent system.

The structure of an R-axial-substituted cobalamin is shown in Figure 1. If the cobalt is Co^{3+}, then the R group should be an anion or carbanion for a neutral molecule. The other negative charges come from the corrin ring and from the phosphate of the nucleotide side chain.

The R group above the plane of the corrin ring is said to be in the β-axial position, and the 5,6-dimethylbenzimidazole (DBz) base below the plane is said to be binding in the α-axial position. Corrinoids are compounds with a corrin ring system, and those corrinoids with a DBz base bound to ribose in the above

(1) Pratt, J. M. In *Chemistry and Biochemistry of B_{12}*; Banerjee, R., Ed.; John Wiley & Sons: New York, 1999; p 104.

10.1021/ja054479c CCC: $33.50

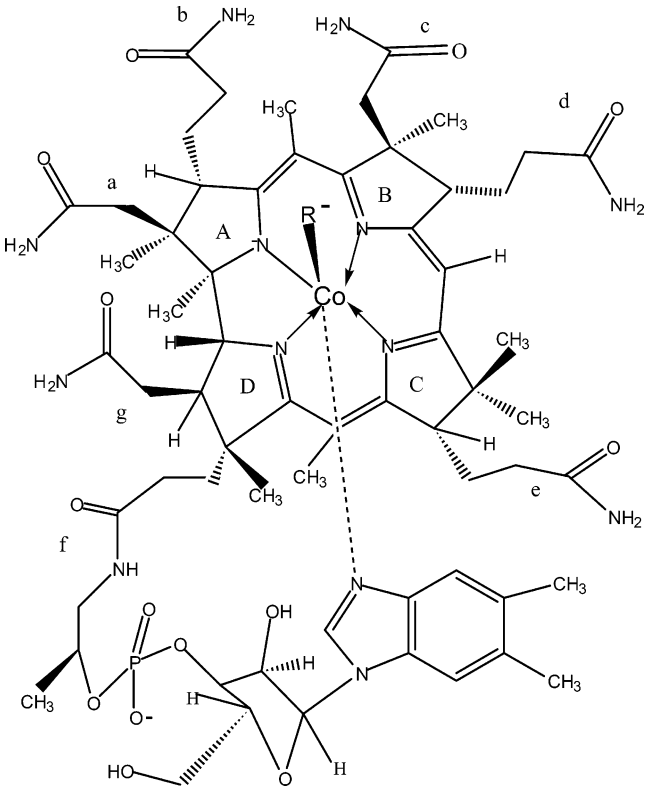

Figure 1. Molecular structure of neutral alkylcobalamin with rings A−D and side chains a−g. In this study, the axial R group is either an alkyl group or an adenosyl group. The Co is in the 3+ oxidation state.

Scheme 1

$$\text{R-Cbl} + e^- \rightleftharpoons [\text{R-Cbl}]^-_{\text{base-on}} \rightarrow \text{R}\cdot + \text{B12s}^-$$
$$\downarrow\uparrow$$
$$[\text{R-Cbl}]^-_{\text{base-off}} \rightarrow \text{R}\cdot + \text{B12s}^-$$

nucleotide side chain are called cobalamins, while those with the nucleotide side chain cleaved with the phosphate group replaced by a C−OH cap are called cobinamides (Cbi). Vitamin B_{12} itself is the cyanocobalamin molecule, so alkylcobalamins can be written as R-B_{12} or R-Cbl.

The mechanism of electroreduction was first studied by Lexa and Savéant[2] for Me-Cbl and methylcobinamide (Me-Cbi) using rapid sweep cyclic voltammetry (CV). Since the electrode process is one-electron overall and B_{12s} is detected electrochemically, the mechanism they proposed was that shown in Scheme 1, where R was the methyl group in their studies and the Co−C bond breaking could come directly from the one-electron adduct with the α-axial DBz base-on, $[\text{R-Cbl}]^-_{\text{base-on}}$, or from a parallel pathway which goes through the α-axial DBz base-off, $[\text{R-Cbl}]^-_{\text{base-off}}$, followed by the irreversible bond-breaking steps. Subsequently, we studied this reaction with Me-Cbl and Ado-Cbl in aqueous media on a mercury electrode at room temperature[3] and in DMSO solvent.[4] Our results indicate that there is a dramatic effect on the cleavage reaction of reduced Me-Cbl on going from an aprotic to an aqueous-surfactant solvent, the reaction in aqueous solvent being around 1000 times slower (see Table 1).

The communication by Lexa and Savéant[2] showed that the reduction potential was shifted from −1.60 V vs SCE to −1.46 V vs SCE on going from Me-Cbl to Me-Cbi. This shift is also consistent with our assignment of base-off and base-on forms in aqueous surfactant solution. The observation of a more positive reduction potential for the base-off form of methylcorrinods is relevant to those B_{12}-dependent enzymes which bind R-Cbl with the 5,6-dimethylbenzimidazole displaced from the corrin ring and replaced by a histidine residue of the protein acting as a ligand to the cobalt ion.[5]

Table 1

species	solvent	temperature	rate constant (s^{-1})
Me-Cbl (ref 2)	1:1 DMF/1-PrOH	−20 °C	1.2×10^3
Me-Cbl (ref 3)	H_2O/triton X-100	rt	0.37
Ado-Cbl (ref 3	H_2O/triton X-100	rt	2.7×10^3
Me-Cbl (ref 4)	DMSO	rt	1.5×10^3

Scheme 2

$$\text{Me-Cbl} + e^- \rightleftharpoons [\text{Me-Cbl}]^- \underset{k_{-1}}{\overset{k_1}{\rightleftharpoons}} \{\text{Me}\cdot + \text{Cbl(I)}^-\}$$
$$+$$
$$\text{Trap}$$
$$\downarrow k_2$$
$$\text{Me-Trap}$$

In the reductive cleavage mechanism, the Co−C bond of the reduced methylcobalamin ([Me-Cbl]$^-$) cleaves homolytically, and Martin and Finke[6] estimate that the rate of the subsequent reaction in the reductive cleavage is enhanced by a factor of ca. 10^{15} at room temperature over the thermal homolysis rate of Me-Cbl in a comparable solvent system. Although this fact might suggest the possibility of an outer-sphere electron-transfer-mediated enzymatic mechanism, this mechanism was ruled out[6] because biological redox agents do not have enough reducing power to overcome the very negative redox potentials found for Me-Cbl (−1.2 to −1.6 vs SCE), even considering possible subsequent exothermic reactions which might drive the endoergic redox process. On the other hand, charged atoms in the enzyme, such as Zn^{2+},[7] and electric fields generated in the enzyme[8] as well as inner-sphere interactions can have a dramatic effect on the energetics and kinetics of electron-transfer (ET) and Co−C bond-breaking reactions.

In their discussion of the mechanism for the reductive cleavage reaction of Me-Cbl in homogeneous solution, Martin and Finke include the effect of radical trapping, as shown in Scheme 2, where Trap is a radical trapping species or trapping solvent and [Me-Cbl]$^-$ is in equilibrium with the caged homolysis products. On the basis of this mechanism, they suggest that the solvent effect is more likely an effect of the solvent acting as a good or bad radical trap. In this mechanism, either the bond-breaking step with rate constant k_1 or the trapping reaction (radical coupling) with the rate constant k_2 can be rate determining. In an aqueous medium, the methyl group is poorly solvated, water is a poor radical trap, and cage escape and/or methyl radical coupling may affect the rate-determining step.[3] In the present study, we show that varying

(2) Lexa, D.; Savéant, J.-M. *J. Am. Chem. Soc.* **1978**, *100*, 3220−3222.
(3) Kim, M.-H.; Birke, R. L. *J. Electroanal. Chem.* **1983**, *144*, 331−350.
(4) Kumar, V.; Birke, R. L. *Anal. Chem.* **1993**, *65*, 8−2436.
(5) (a) Dreenan, C. L.; Huang, S.; Drummond, J. T.; Mathews, R. G.; Ludwig, M. L. *Science (Washington, D.C.)* **1994**, *266*, 1669. (b) Mancia, F.; Keep, N. H.; Nakagawa, A.; Leadlay, P. F.; McSweeney, S.; Rasmusssen, B.; Bosecke, P.; Diat, O.; Evans, P. F. *Structure* **1996**, *4*, 339.
(6) Martin, B. D.; Finke, R. G. *J. Am. Chem. Soc.* **1992**, *114*, 585.
(7) Goulding, C. W.; Mathews R. G. *Biochemistry* **1997**, *36*, 15749.
(8) Andruniow, T.; Zgierski, M. Z.; Kozlowsky, P. M. *Chem. Phys. Lett.* **2000**, 509−512.

the dielectric nature of a mixed nonaqueous solvent system can have a significant effect on the rate of the subsequent reaction.

Some of the steps for methyl transfer in vitamin B_{12}-dependent enzymatic reactions, such as in methionine synthase, have their counterpart in the EC reductive cleavage reaction. The enzymatic pathway involves transfer of the Me group from Me-Cbl to the sulfur atom of homocysteine (Hcy), $H_2NCH(COOH)(CH_2)_2$-SH, to form methionine, $H_2NCH(COOH)(CH_2)_2$-S-CH_3. One role of the Zn^{2+} in the enzyme is to bind Hcy, yielding a thiolate which is essential for catalytic activity.[7] Model studies of Me-Cbl with mercaptoethanol in basic solution indicate an S_N2-type nucleophilic substitution reaction for the mechanism of this type of reaction.[9] However, there are several possible mechanisms for methyl transfer from Me-Cbl to the thiolate of Hcy which were recently discussed by Matthews,[10] including a reductive cleavage mechanism. Thus, the transition state in the enzymatic mechanism may be related to the electronic structure of the radical anion $[Me\text{-}B_{12}]^-$ formed in the EC reductive cleavage process and located along the pathway for Co−C bond breaking.

The previous studies of Co−C bond breaking following ET in Me-Cbl[2−4] all indicate that the process is a stepwise dissociative ET mechanism because they show the existence of the radical anion species. Savéant[11] has developed a semiclassical theory of concerted dissociative electron transfer based on the Morse curve approximation of the potential energy of the breaking bond and a Marcus−Hush solvent reorganization energy. A substantial literature on the transition between the concerted and stepwise types of dissociative ET processes has now developed.[12] For the most part, these studies have involved frangible carbon−halide or carbon−sulfur σ bonds in small organic compounds. Similar considerations for compounds containing an organometallic σ bond have not been made, and the present study of alkylcobalamins is one of the first in this context.

There is a significant difference between simple organic compounds, like the aryl halides, and the alkylcobalamins for a stepwise dissociative mechanism which goes through a radical anion. For aryl halides, the initial ET is to a π^* lowest unoccupied molecular orbital (LUMO) situated in the aryl group, and the π^* bound state crosses the dissociative σ^* state at an avoided crossing, which leaves the electron in the halide and gives an aryl radical on bond breaking.[12d,e,13] On the other hand, for the alkylcobalamins, the aromatic system is in the corrin ring of the cobalamin, which appears to directly receive the electron in the π^* LUMO, as discussed below, and which retains the negative charge on bond breaking to form $Cbl(I)^-$, B_{12s}^-, and the radical, $R^\bullet$. However, the energetics may be quite similar since the intramolecular ET must lead to a dissociative state which crosses the bound state in an avoided crossing, leading to an adiabatic curve with a lower activation energy. A detailed review of intramolecular dissociative ET has recently considered various types of intramolecular processes.[14] Both organic C−X and C−Co bond-breaking mechanisms must involve intramolecular ET from orbitals of different symmetry, which also may require some contortion in the transition state.[13,14]

Since the radical anion ($[Me\text{-}Cbl]^-$) formed electrochemically dissociates through a set of consecutive steps and not in a concerted manner, the alkylcobalamin radical anion species formed should not initially have the $(\sigma)^2\sigma^*$ weakened three-electron bond originally suggested as a configuration necessary prior to Co−C bond cleavage.[15] This suggestion was based on low-level calculations which predicted that the LUMO was a Co−C antibonding σ^* orbital.[15] In fact, more recent semiempirical PM3 calculations[16] and density functional theory (DFT) calculations[17] both with the actual Co-corrin ring and with an imidazole axial base as a model show that the LUMO is a π^* antibonding corrin ring molecular orbital (MO) with a slight contribution from a cobalt $3d_{yz}$ orbital. Unfortunately, geometry-optimized calculations for the entire Me-Cbl compound (183 atoms, 506 electrons) as well as for ethyl-, *n*-propyl-, *n*-butyl-, 2-butyl-, and adenosylcobalamins would require large amounts of memory and CPU time and have not been done to date. However, density functional theory (DFT) calculations have been made for models of Co-corrin compounds, typically with all side chains of the cobalamin ring replaced with hydrogen. The model DFT calculations in the literature show that the Co−C σ^*-containing MO is several electronvolts above the LUMO. It is, in fact, the LUMO(+4) in Me-Cbl but is significantly lowered to the LUMO(+3) in the base-off Me-Cbi.[17]

Those calculations and the ones we will report herein indicate that weakening of the lower axial base bonding to the Co ion, which lowers the σ^* MO, is important for achieving a low-energy pathway in the dissociative ET mechanism for the Co−C bond breaking in alkylcobalamins. This is also consistent with a >1500-fold increase in the rate constant for protein free methyl transfer to an RS^- acceptor for Me-Cbi over Me-Cbl.[1] The mechanistic pathway that will be explored in this paper for the EC cleavage requires going through a step to form the base-off cobalamin species and then an intramolecular ET to eventually form a $(\sigma)^2\sigma^*$ weakened three-electron bond. In fact, the cage species of Scheme 2 can be described as either a charge−dipole interaction or a σ anion radical with a very long Co−C bond formed by a weak three-electron bond.[18] Thus, this stepwise pathway involves a dissociation of the side-chain DBz base as well as an intramolecular ET from a π^* to a σ^* electronic state of the radical anion at an avoided crossing. The latter step appears to involve a conical intersection and/or vibronic interactions.

Herein, we report measured EC potentials and an estimation of entropy parameters which allows a calculation of the

(9) Hogenkamp, H. P. C.; Bratt, G.; Sun, S.-Z. *Biochemistry* **1985**, *24*, 6428.
(10) Matthews R. G. *Acc. Chem. Res.* **2001**, *34*, 681−689.
(11) Savéant, J.-M. *J. Am. Chem. Soc.* **1987**, *109*, 6788.
(12) (a) Andrieux, C. P.; Gorande, A. L.; Savéant, J.-M. *J. Am. Chem. Soc.* **1992**, *114*, 6892−6904. (b) Savéant, J.-M. *J. Phys. Chem.* **1994**, *89*, 3716−3724. (c) Savéant, J.-M. *Acc. Chem. Res.* **1993**, *26*, 455−461. (d) Savéant, J.-M. *Adv. Phys. Org. Chem.* **2000**, *35*, 117−192. (e) Maran, F.; Wayner, D. D. M.; Workintin, M. S. *Adv. Phys. Org. Chem.* **2001**, *36*, 85. (f) Mariano, D.; Vera, A.; Pierini, A. B. *J. Phys. Org. Chem.* **2002**, *15*, 894−902. (g) Antonello, S.; Benassi, R.; Gavioli, G.; Taddei, F.; Maran, F. *J. Am. Chem. Soc.* **2002**, *124*, 7529−7538.
(13) Takeda, N.; Poliakov, P. V.; Cook, A. R.; Miller, J. R. *J. Am. Chem. Soc.* **2004**, *126*, 4301−4309.
(14) Antonello, S.; Maran, F. *Chem. Soc. Rev.* **2004**, *34*, 418.
(15) Finke, R. G.; Martin, B. D. *J. Inorg. Biochem.* **1990**, *40*, 19−22.
(16) Cole, A. G.; Yoder, L. M.; Shiang, N. A.; Anderson, N. A.; Walker, L. A., II; Banaszak Holl, M. M.; Sension, R. J. *J. Am. Chem. Soc.* **2002**, *124*, 434−441 (molecular orbitals in Supporting Information).
(17) Stich, T. A.; Brooks, A. J.; Buan, N. R.; Brunold, T. C. *J. Am. Chem. Soc.* **2003**, *125*, 5897−5914.
(18) (a) Pause, L.; Robert, M.; Savéant, J.-M. *J. Am. Chem. Soc.* **2000**, *122*, 9829−9835. (b) Pause, L.; Robert, M.; Savéant, J.-M. *J. Am. Chem. Soc.* **2001**, *123*, 11908−11916. (c) Costentin, C.; Robert, M.; Savéant, J.-M. *J. Am. Chem. Soc.* **2003**, *125*, 10729−10729. (d) Costentin, C.; Robert, M.; Savéant, J.-M. *J. Am. Chem. Soc.* **2004**, *126*, 16834−16840.

equilibrium bond dissociation enthalpy for Co−CH_3 in Me-Cbl and its radical anion. We use a digital simulation technique and the theory of the EC process to measure thermodynamic reduction potentials for the heterogeneous ET reaction to form the radical anion. This simulation−curve-fitting of the cyclic voltammetry data is used for Me-Cbl as well as for a series of other alkylcobalamin compounds. Because of the stepwise nature of the electrode process, the kinetics and thermodynamics of the initial ET can be separated from the thermodynamics of the bond dissociation step. This separation allows the use of the Marcus−Hush−Levich theory of electron transfer to show that the initial ET step is nonadiabatic and to estimate the electronic coupling matrix element from the data for Me-Cbl with nonadiabatic ET theory. We also measure the kinetics of C−Co bond breaking for Me-Cbl experimentally by double-potential-step chronoamperometry as a function of temperature and solvent mixtures.

In a previous EC study of a series of alkylcobalamins,[19] the peak potentials of a large variety of axial groups were measured by forming the Co−R bond in situ starting from aquocobalamin and an organic halide. The compounds formed by an electrocatalytic cycle at the electrode surface. Potentials found in this way were not considered to give thermodynamic E° values,[19] and in the present paper we improved on this study by doing the electrochemistry on members of the alkylcobalamin series made by chemical synthesis. The effect of the various alkyl groups on the reduction potentials obtained and on the bond-breaking reaction is interpreted in terms of DFT electronic structure calculations. A correlation of C−Co bond distance with redox potential is made with DFT calculations for this series of alkyl groups. Finally, the effect of the solvent environment on the Co−C cleavage rates for Me-Cbl is considered.

Experimental Section

Chemicals. Methylcobalamin and hydroxocobalamin were obtained from Sigma-Aldrich. Cobalt nitrate, sodium borohydride, ethyl iodide, *n*-propyl iodide, *n*-butyl iodide, and isobutyl iodide were the purest forms available from Aldrich. Tetrabutylammonium fluoroborate (TBAF), *N*,*N*-dimethylformamide (DMF), methanol, pentane, and ethyl acetate were obtained from Fisher Scientific. All solvents were reagent grade. Water was purified by a deionizing system followed by distillation. TBAF was purified by first dissolving in ethyl acetate, filtering, and then recrystallizing by dropwise addition of pentane. The crystal form of TBAF was washed twice with pentane. The recrystallization procedures were repeated twice. The crystallized TBAF was finally dried under vacuum at room temperature. DMF was filtered and distilled twice under reduced pressure at about 30 °C. Methanol was filtered and distilled twice under regular pressure at about 64 °C. To treat the water remaining in methanol, I_2 and metal Mg were added in an evaporating flask; 3-Å molecular sieves (Alfa) were finally used to adsorb the remaining trace amount of water in DMF and methanol. The procedure for preparation of the alkylcobalamins is given in the Supporting Information.

Electronic Structure Calculations. The semiempirical calculations were made with the PM3 method using the Spartan '04 program (Wavefunction, Inc.). Density functional theory calculations were made with the 2003 version[20] of the GAUSSIAN suite of programs (Gaussian, Inc.) with the NCSA Xeon Cluster supercomputer.

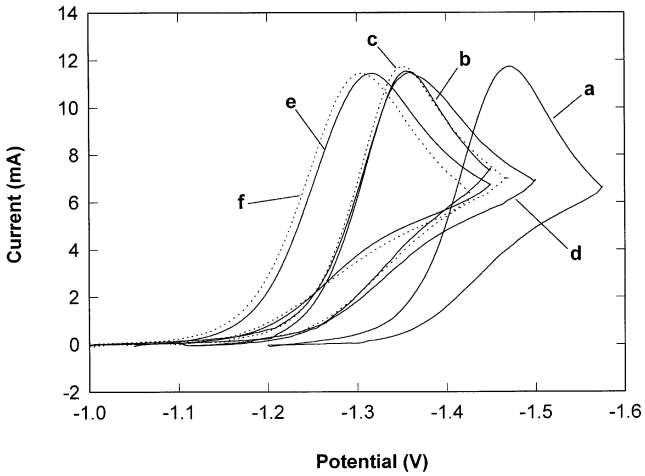

Figure 2. Cyclic voltammograms of alkylcobalamins at 20 °C. Current is in microamperes, potential is vs the nonaqueous Ag/AgCl reference. Experiments were performed with a 1.6 mm silver amalgam electrode in a solvent mixture of DMF and methanol (40:60) at a scan rate of 300 mV/s in 0.20 M TBAF with each alkylcobalamin at 2.0 mM: (a) methylcobalamin, (b) ethylcobalamin, (c) *n*-propylcobalamin, (d) *n*-butylcobalamin, (e) isobutylcobalamin, and (f) adenosylcobalamin.

Apparatus and Procedures. Electrochemical experiments were performed with a BAS-100A electrochemical analyzer (Bioanalytical Systems) or a CH 660A workstation (CH Instruments). A three-electrode configuration was employed for all experiments. For experiments performed in nonaqueous media, the reference electrode was an Ag/AgCl/chloride nonaqueous electrode (Metrohm, Herisau, Switzerland) with the ethanol solvent saturated by LiCl (ultrapure grade, Alfa) at −85 °C, the lowest temperature the temperature control system could reach. This electrode was found to be 0.049 V positive to an aqueous Ag/AgCl/chloride (3 M) electrode (BAS). The counter electrode was platinum wire (d = 0.5 mm). The silver amalgam working electrodes were made on silver electrodes (d = 1.6 and 0.50 mm) and were described previously.[21,22] Some experiments were made on a mercury drop working electrode using a BAS controlled-growth mercury electrode (CGME) in the SMDE mode. The distance between the working and reference electrodes was kept to a minimum in order to minimize the uncompensated resistance. The EC cell was shielded from light and electromagnetic field and was immersed in coolant ethanol for low-temperature studies. The cell temperature was monitored by an Omega temperature probe near the working electrode and was controlled by a temperature bath controller (FTS systems) with a precision of ±1 °C. The media were solvent mixtures of DMF and methanol with supporting electrolyte TBAF. The solutions were prepared at room temperature, so the molar concentrations pertain to about 24 °C. Prior to experiments, solutions were purged with nitrogen for at least 15 min and a nitrogen atmosphere was then maintained over the solutions during the course of experiments. The purge nitrogen was presaturated with the same solvent mixtures as used in the experiment and precooled to the working temperature through a U-tube immersed in the coolant ethanol.

Results and Discussion

Cyclic Voltammetry of Alkylcobalamins. Cyclic voltammograms of alkylcobalamins show similar CV curve shapes but different peak potentials in a solvent mixture of DMF and methanol (40:60) at 20 °C (Figure 2). With the same scan rate of 300 mV/s, they have peak potentials of −1.47 V for methylcobalamin, −1.36 V for ethylcobalamin, −1.35 V for *n*-propylcobalamin, −1.36 V for *n*-butylcobalamin, −1.32 V

(19) Zhou, D.-L.; Tinembart, O.; Scheffold, R.; Walder, L. *Helv. Chim. Acta* **1990**, *73*, 2225.
(20) Frisch, M. J.; et al. *Gaussian 03*, Revision B.05; Gaussian Inc.: Pittsburgh, PA, 2003.
(21) Huang, Q.; Gosser, D. K. *Talanta* **1992**, *9*, 1155.
(22) Huang, Q.; Rusling, J. F. *Environ. Sci. Technol.* **1995**, *29*, 98.

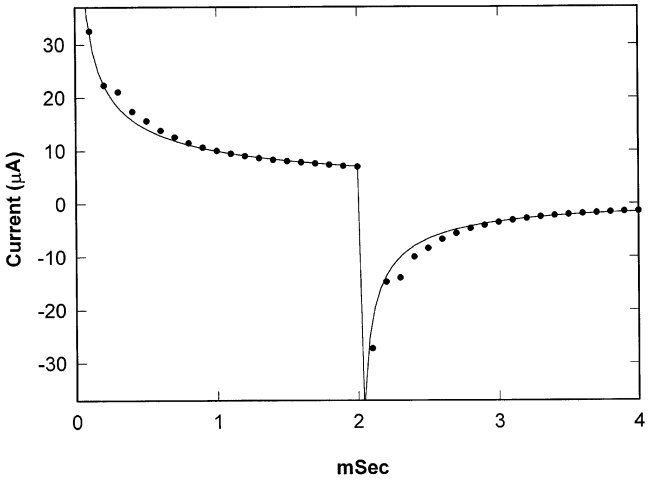

Figure 3. Current vs time in a DPSC experiment. Data and curve-fitting results for methylcobalamin in a solvent mixture of DMF and methanol (50:50) at −40 °C. Experiments were performed with a 0.50 mm silver amalgam working electrode; methylcobalamin 2.0 mM in 0.20 M TBAF. Initial potential, −1300 mV, potential step to −1600 mV for 2 ms, and final potential, −1300 mV. The simulated theoretical curve has a 90 s^{-1} rate constant for the reaction. The solid dots represent the experimental data.

for isobutylcobalamin, and −1.31 V for adenosylcobalamin. All potentials are against a nonaqueous Ag/AgCl reference electrode. The difference in these alkyl groups seems be related to a steric effect between the alkyl group and the methyl and/or hydrogen on the corrin ring, mainly coming from the β carbon of the alkyl. With this reasoning, ethyl, *n*-propyl, and *n*-butyl groups would seem to have similar steric effects and show close peak potentials. 2-Butylcobalamin and adenosylcobalamin have a more branched structure, and their peak potentials are more positive than those of the straight-chain alkyl substituents. In fact, they show the most positive reduction peaks of our group of alkylcobalamins. The reason for the order of these peak potentials will be considered in terms of a detailed mechanism of the electrode process and electronic structure calculations discussed later.

Double-Potential-Step Chronoamperometry. Double-potential-step chronoamperometry (DPSC) was used to measure the rate constant k_{chem} for the irreversible reaction by stepping the potential from −1.3 to −1.6 V vs the Ag/AgCl nonaqueous reference electrode. One example of the chronoamperometric experiments in given in Figure 3. From a series of DPSC experiments, a plot of rate constant versus temperature for Me-Cbl in two different solvent mixtures of DMF/methanol (40:60 and 50:50) was made (Figure 4). It is interesting to compare rate constants at −20°C for different solvent mixtures: for the 40:60 mixture, $k_{chem} = 1.2 \times 10^3$ s^{-1} and for the 50:50 mixture, $k_{chem} = 3.6 \times 10^2$ s^{-1}, whereas in a 50:50 mixture of DMF/2-propanol, a value of $k_{chem} = 1.2 \times 10^3$ s^{-1} was found.[2] It appears that both the alcohol type and content of the solvent mixture have an effect on this rate constant. The rate constant for the reaction (k_{chem}) of Me-Cbl in a solvent mixture of DMF/MeOH (40:60) was estimated as 5.5×10^3 s^{-1} at 20 °C. Ethyl-, *n*-propyl-, *n*-butyl-, isobutyl-, and adenosylcobalamins have much faster reaction rates, and estimation of them at 20 °C was beyond the scope of these experiments.

It appears as if the rate of the reaction of Me-Cbl in DMF/MeOH is very sensitive to the polarity of the solvent mixture (Figure 4). The rate is faster in the solvent mixture of

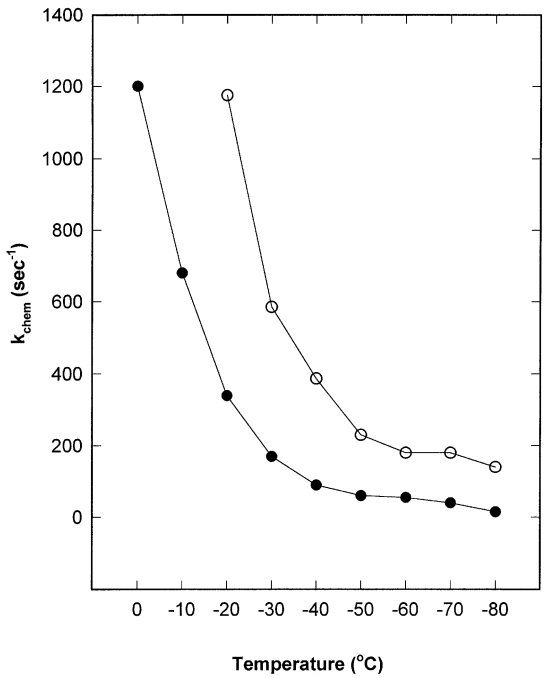

Figure 4. Rate constants of the reaction of methylcobalamin in two solvent mixtures as a function of temperature: DMF/MeOH (a) 40:60 (○) and (b) 50:50 (●); 0.50 mm silver amalgam working electrode; methylcobalamin 2.0 mM in 0.20 M TBAF.

DMF/methanol (40:60) than in the 50:50 mixture over the entire temperature range from 0 to −80 °C. The reaction rate generally decreases as the temperature is lowered. However, the change levels off around −50 °C for the 50:50 DMF/MeOH mixture and around −60 °C for the 40:60 mixture. On continued decreasing of the temperature, the reaction rate resumes decreasing. It has been reported that a cyclic DMF dimer forms at low temperature which has minimal steric interaction and enhances charge delocalization by forming a chairlike six-membered ring.[23] Therefore, this DMF dimerization should lower the polarity of the solvent mixture. On the other hand, the mole ratio of methanol is increased by this dimerization, and it appears that the dielectric constant of methanol is dramatically increased at lower temperature. For example, $D = 33.1$ at 20 °C, 37.1 at 0 °C, 41.5 at −20 °C, 48 at −50 °C, and 54 at −80 °C.[24] The data in Figure 4 allow a plot (Figure 5) of an Arrhenius-type relationship to be made which was extended from low temperature to 20 °C.

The activation enthaplies of the reaction were calculated from the slope of $\ln_e(k_{chem}/T)$ vs $1/T$ in a linear region of the plot, i.e., from 220 to 273 K. The results of a linear fit in this region give $\Delta H = 5.8 \pm 0.5$ kcal/mol and 7.6 ± 0.3 kcal/mol, with pre-exponential factors $A/T = (4.0 \pm 3.0) \times 10^5$ and $(5.6 \pm 1.7) \times 10^6$ s^{-1} in the solvent mixtures of 40:60 and 50:50 DMF/MeOH, respectively. These results could indicate that the activation free energy of the reaction of Me-Cbl shown in Scheme 2 is related to either the polarity of the solvent mixture (i.e., by solvation or reorganization) or the trapping effectiveness of the solvent mixture, or both. Again, these results will be

(23) Van Duyne, R. P.; Reilly, C. N. *Anal. Chem.* **1972**, *44*, 142.
(24) (a) *CRC Handbook of Chemistry and Physics*, 68th ed.; CRC Press: Boca Raton, FL, 1987−88. (b) *International Critical Tables of Numerical Data, Physics, Chemistry and Technology*, 1st electronic ed.; Washburn, E. W., Ed.; Knovel: 2003 (http://www.knovel.com/knovel2/Toc.jsp?BookID=735&VerticalID=0).

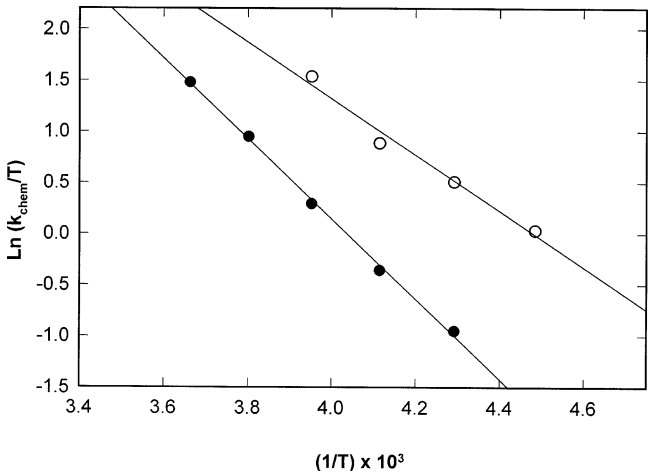

Figure 5. Plot of ln(k_{chem}/T) vs 1/T in the temperature range of "normal" behavior in Figure 4. The solvent mixtures of DMF/MeOH are (a) 40:60 (○) and (b) 50:50 (●).

discussed after a detailed mechanism is considered for bond cleavage.

Simulation−Fitting of the Cyclic Voltammograms of Methylcobalamin. According to the Butler−Volmer equation,

$$i = nFAk^{\circ}\left\{C_O(0,t)\exp\left[-\alpha nF\left(\frac{E-E^{\circ\prime}}{RT}\right)\right] - C_R(0,t)\exp\left[(1-\alpha)nF\left(\frac{E-E^{\circ\prime}}{RT}\right)\right]\right\} \quad (1)$$

where the parameters have their usual meaning,[26] an electroreduction process becomes totally irreversible when the second term, related to $C_R(0,t)$, can be ignored. In this case, the EC parameters apparent standard heterogeneous rate constant, charge-transfer coefficient, and apparent redox potential, k°, α, and $E^{\circ\prime}$, respectively, cannot be determined through a simulation. This situation results because an unlimited combination of k° and $E^{\circ\prime}$ can be obtained from the same voltammogram in a totally irreversible system since

$$\ln k^{\circ} + \alpha nE^{\circ\prime}/RT = \text{constant} \quad (2)$$

However, curve-fitting of a cyclic voltammogram by simulation to determine these three parameters in an EC process can still be used if the mechanism involves a quasi-reversible electrode reaction.[21,25] In a region where k° is so small that the system is totally irreversible, exactly the same cyclic voltammogram is obtained, even when the value of k° is changed by several orders of magnitude. However, when the EC system is not totally irreversible, the second term in the Butler−Volmer equation begins to influence the current in the voltammogram. The useful region for such parameter fitting can be estimated by determining through simulation where the current−voltage curve is still influenced by quasi-reversible electrode kinetics. The peak potential calculated from simulation of the EC mechanism is then a function of k°. The measurement of α and the error estimate in such a quasi-reversible system have been discussed.[21] For a totally irreversible system, the EC coefficient α can be measured independently.[26]

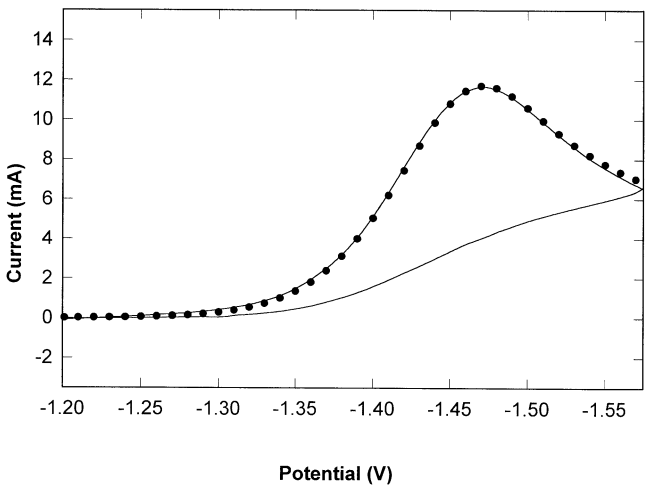

Figure 6. Cyclic voltammogram of methylcobalamin at 20 °C and the simulation−fitting results. Current is in microamperes, potential is vs nonaqueous Ag/AgCl reference. Experiments were performed with a 1.6 mm silver amalgam electrode in a solvent mixture of DMF and methanol (40:60) at a scan rate of 300 mV/s; methylcobalamin 2.0 mM in 0.20 M TBAF. $k_{chem} = 5.5 \times 10^3$ s^{-1}; solution resistance of 660 Ω, and diffusion coefficient of 4.1×10^{-6} cm^2/s were used in simulation−fitting. The curve represents experimental data, and the dots represent the simulation−fitting results.

The CV simulations and curve-fitting in the present paper were done with the CVSIM and CVFIT programs discussed in ref 25. The results of a simulation study of the EC mechanism indicate that the EC reaction of Me-Cbl, with a subsequent reaction rate constant of 5.50×10^3 s^{-1} at 20 °C, will be in a k°-dependent region if $k^{\circ} > 4 \times 10^{-3}$ cm/s. This situation is for a simple EC mechanism (three chemical species) with a single one-electron quasi-reversible EC step and a single subsequent chemical step. When a rate constant of 5.50×10^3 s^{-1}, found by DSPC for the subsequent reaction, is used as an input parameter in simulation−fitting of this EC mechanism for our CV experimental data at 20 °C, we get the dots on the experimental curve shown in Figure 6.

The curve-fitted EC parameters found are $E^{\circ\prime} = -1.466$ V, $k^{\circ} = 0.016$ cm/s, and $\alpha = 0.77$. A scan rate study of the above system at room temperature over the range 0.3−200 V s^{-1} shows no return wave and a shift of peak potential of −0.023 V per decade of scan rate. Both peak potential and scan rate were corrected for the effects of uncompensated resistance. The corrected $E_p - E_{p/2} = 0.061$ V for Figure 6 and the value of the shift of −0.023 V per log scan rate, which is close to the expected value of −0.029 V, show that the process is a stepwise mechanism[29] with controlled by both the ET reaction and the steps that follow.

The determined charge-transfer coefficient of Me-Cbl is nearly the same as the value measured at −30 °C ($\alpha = 0.78$) in the same solvent mixture.[21] These results suggest that the temperature will not change the EC mechanism for Me-Cbl in the solvent mixture of DMF and methanol. The k° of Me-Cbl in the same solvent mixture at −30 °C was determined previously as 0.012 ± 0.002 cm/s.[21]

A Detailed Electrode Process for Methylcobalamin Reduction. At the slow scan rate of 0.3 V/s used in the above

(25) (a) Gosser, D. K., Jr. *Cyclic Voltammetry−Simulation and Analysis of Reduction Mechanisms*; VCH: New York, 1993. (b) Gosser, D. K., Jr.; Rieger, P. H. *Anal. Chem.* **1988**, *60*, 1159.
(26) Bard, A.; Faulkner, L. *Electrochemical Methods, Fundamentals and Applications*, 2nd ed.; Wiley: New York, 2001.
(27) Brown, K. L.; Peck-Siler, S. *Inorg. Chem.* **1988**, *27*, 3548−3555.
(28) Marcus, R. A. *Annu. Rev. Phys. Chem.* **1964**, *15*, 155−196.
(29) Savéant, J.-M. *Adv. Phys. Org. Chem.* **1990**, *26*, 1−130.

Scheme 3

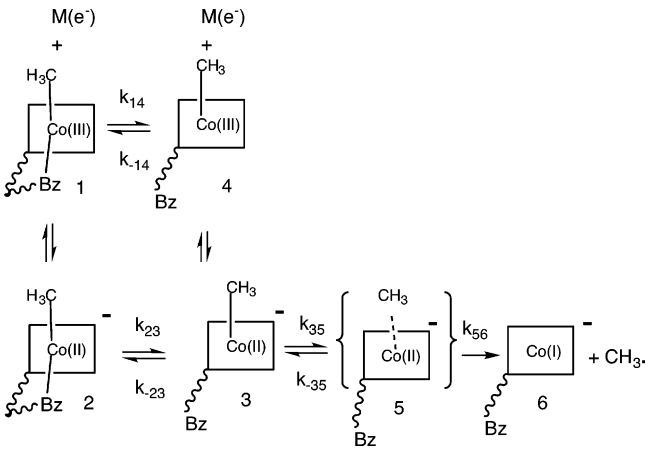

simulation experiment, the CV of Me-Cbl has no return wave; however, as the scan rate is increased to 10 V/s and above at −20 °C, a return wave appears, which allowed Lexa and Savéant[2] to propose the multistep EC mechanism given in Scheme 1. In our above analysis, we have implicitly assumed that all equilibrium steps that follow the charge-transfer step are in rapid equilibrium (quasi-equilibrium assumption), which collapses these steps into a single subsequent reaction at slow scan rates. We can show that this is reasonable for a multistep EC mechanism very similar to but slightly modified from that discussed by Lexa and Savéant.[2] These authors propose that both a base-on and a base-off one-electron adduct, $[Me\text{-}Cbl]^-$, is involved in the mechanism (Scheme 1) and that both species can be reoxidized at a fast scan rate, as observed by the appearance of two merged peaks in the anodic return wave. In fact, this means that the mechanism includes a base-off parent Me-Cbl species which is at very low concentration with respect to the base-on Me-Cbl since there is only one forward reduction wave. This gives a scheme of squares with two electrode reactions (see Scheme 3), which were not explicitly expressed in Scheme 1.

Furthermore, our DFT vacuum calculations of the one-electron-reduced methylcobalamin model show that the activation energy barrier for base-on $[Me\text{-}Cbl]^-$ bond breaking is 0.5 eV higher than for the base-off species, and thus we have not included the bond-breaking reaction from the base-on reduced species in our detailed mechanism in Scheme 3. Finally, we have incorporated the additional equilibrium of a caged homolysis product, species **5**, which is in equilibrium with base-off species **3** ($[Me\text{-}Cbl]^-$), as in Martin and Finke's mechanism[6] shown in Scheme 2. We have simulated CV curves as a function of scan rate for the detailed mechanism in Scheme 3.

Figure 7 shows the results of the simulations which best match the experimental curves of Lexa and Savéant at 253 K for the electroreduction of Me-Cbl (Figure 2 of ref 2). In these simulations we fixed the E° parameters for the two-electrode reactions and k_{chem} as those given by Lexa and Savéant,[2] and we used values of the heterogeneous rate parameters consistent with the value we found in the simulation−curve-fitting of our slow-scan data. The homogeneous equilibrium constants (with fast kinetic rates) were varied for the reversible steps in Scheme 3 (see Figure S1 for the method of evaluation of K_{23} and K_{35}) to give voltammograms that agree with the peak voltages (within ±0.01 V) and approximate anodic-to-cathodic current ratios in the data of Lexa and Savéant at the various scan rates of 5, 10, 20, 50, 100, and 200 V/s (Figure 7). A comparison of the simulated curves in Figure 7 with the fast-scan data in ref 2 shows that all the qualitative features of the experimental CV curves are reproduced; i.e., there is one sharp peak on the forward scan and a broad peak on the reverse scan with about 1:4 anodic-to-cathodic peak current ratio, as measured from each baseline (at 200 V s^{-1}), and this broad return wave, $E_p{}^a = -1.40$ vs SCE, appears only at scan rates higher than about 10 V/s. With the parameter values used in the simulation of Scheme 3, there is a stationary state for species **3** and **5**, and the overall rate constant for bond breaking is approximated by $k_{chem} = k_{56}K_{23}K_{35} = 1.2 \times 10^3\ s^{-1}$.

In terms of the equilibrium constants used in the above simulation, K_{14} and K_{23} have the smallest uncertainty, while K_{35} is the most uncertain. The value for the base-on/base-off equilibrium constant K_{14} which was used is 5 times larger than an extrapolation to 253 K of the NMR results for Me-Cbl in aqueous solution,[27] which gives $K_{14} = 2.0 \times 10^{-4}$. However, the larger value is consistent with the nature of the solvent, since DMF is a better ligand than water for hexacoordinate Co(III). In fact, the simulation gives the same curves for any K_{14} lower than 1×10^{-3}. For larger K_{14} values, the two ET steps would begin to influence the forward scan. This analysis gives only approximate estimates of K_{23} and K_{35} (see discussion of Figure S1); however, even though their values are uncertain, they allow error bars to be put on the bond dissociation enthalpy of Me-Cbl, which is calculated later.

If we directly compare a simulation of the multistep mechanism with that of a simple EC mechanism (quasi-reversible electrode − single subsequent chemical step), using the same heterogeneous parameters and a steady-state value of k_{chem} in the EC case and above values in the multistep case, the curves in the forward scan direction overlap exactly at each scan rate simulated (Figure S2) from 0.3 to 200 V/s. A plot of the peak potential vs log(scan rate) of the data in Figure S2 gives −23 mV/decade, which is close to what is found experimentally in our room-temperature study. Thus, as expected, the standard potential of the single ET step to form the base-on radical anion, $E^\circ{}_{12}$, along with the other heterogeneous parameters and the rate constants of the subsequent chemical steps control the peak potential and shape of the CV curve in the forward scan direction in both mechanisms.

The Nonadiabatic Nature of the Electron-Transfer Step for Methylcobalamin Reduction: Calculation of the Electronic Coupling Matrix Element. It is of interest to determine whether the ET is adiabatic or nonadiabatic since this will indicate whether there is strong (adiabatic) or weak (nonadiabatic) coupling of the delocalized metallic state of the electron in the electrode with a localized acceptor orbital of Me-Cbl, which should be the π^* LUMO of the corrin ring. This determination can be made by comparing the measured $k^\circ{}_{12}$ with a value calculated from the Marcus−Hush theory of outer-sphere adiabatic ET. One form of this theory[28] starts from a transition-state-type rate constant expression for ET,

$$k_i = Z\kappa\rho\ e^{-\Delta G_i^*/RT} \qquad (3)$$

where following Marcus,[28] Z is the collision frequency per unit area of the electrode, κ is the transmission coefficient (a nuclear-velocity-weighted average transmission probability), ρ is the

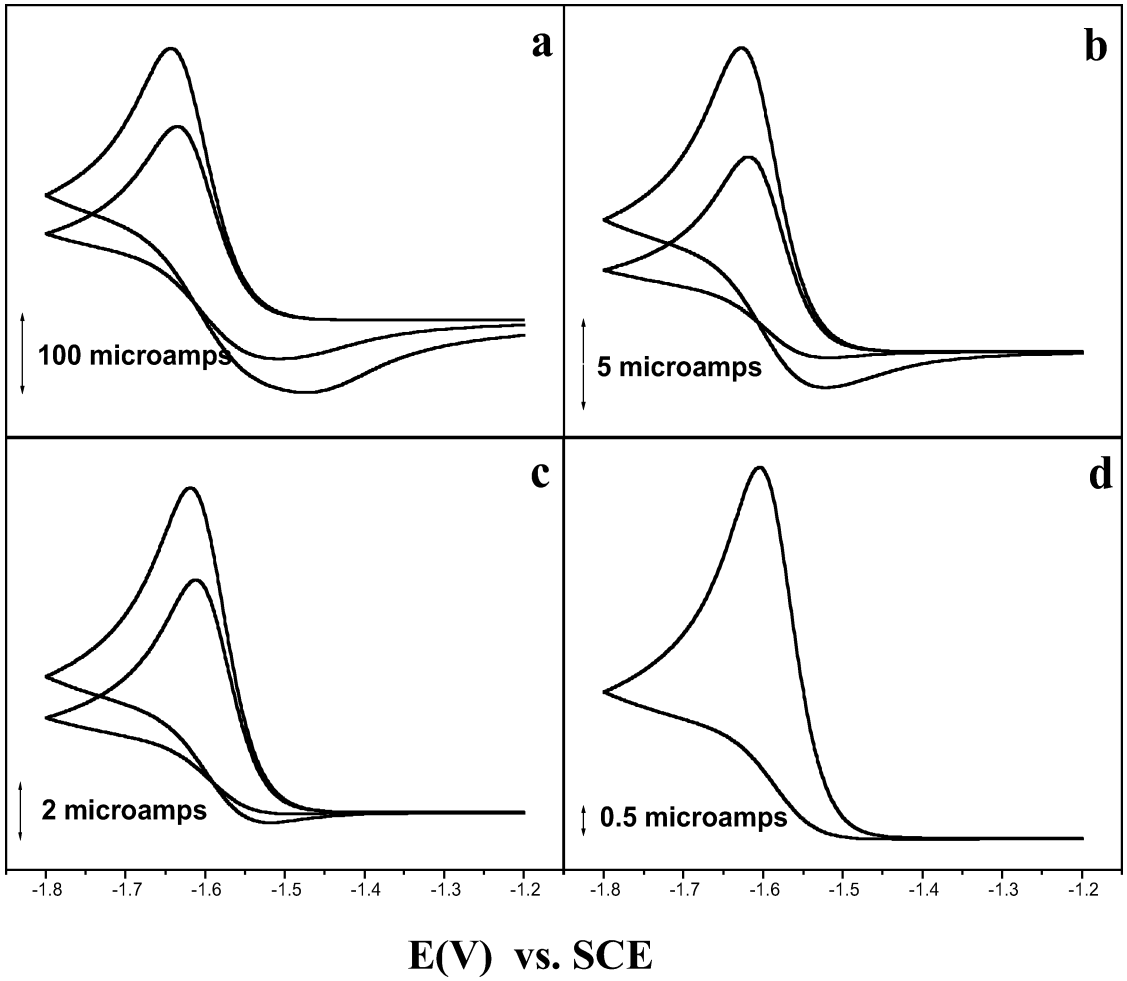

Figure 7. Digital simulation of the cyclic voltammetry curves reported by Lexa and Savéant (Figure 2, ref 2). Simulated CV curves of methylcobalamin at −20 °C, 1:1 DMF/1-propanol; supporting electrolyte, NBu_4BF_4 (0.1 M); reference electrode, aqueous SCE; potential range from −1.2 to −1.8 V. Sweep rates (V s^{-1}): (a) 200, 100; (b) 50, 20; (c) 20, 10; (d) 5. Simulation parameters: $E^{\circ}_{12} = -1.60$ V, $E^{\circ}_{43} = -1.47$ V, $k^{\circ}_{12} = 0.10$ cm/s, $\alpha = 0.7$, $k^{\circ}_{43} = 0.10$ cm/s, $\alpha = 0.5$, $K_{14} = 1.0 \times 10^{-3}$, $K_{23} = 2.0$, $K_{35} = 0.1$, $k_{56} = 6.0 \times 10^3$ s^{-1}, giving $k_{chem} = 1.2 \times 10^3$ s^{-1}.

ratio of fluctuation distances in the activated complex, which was taken as unity, and ΔG_i^* is the activation free energy for a cathodic (i = c) or anodic (i = a) process; the other symbols have their usual meanings. For $\kappa \approx 1$, the ET is adiabatic, and for $\kappa \ll 1$, it is nonadiabatic. If the value of κ extracted from the measured rate constant is much less than unity, then the nonadiabatic nature of the electron process and thus weak electronic interaction is established.

The activation energies derived in Marcus−Hush theory are quadratic functions of the standard free energy, $\Delta G^{\circ} = G^{\circ}_R - G^{\circ}_P = nF(E - E^{\circ\prime})$, for the ET reaction and can be expressed[28,29] as

$$\Delta G_c^* = w_r + \frac{\lambda}{4}\left\{1 + \frac{\Delta G^{\circ} - w_r + w_p}{\lambda}\right\}^2 \qquad (4)$$

$$\Delta G_a^* = w_p + \frac{\lambda}{4}\left\{1 - \frac{\Delta G^{\circ} - w_r + w_p}{\lambda}\right\}^2 \qquad (5)$$

where w_r and w_p are reactant and product work terms required to move the reactant to the electrode surface from the bulk solution and vice versa for the product, and λ is sum of the solvent (outer) and internal (inner) reorganization energies. For Me-Cbl, our electronic structure calculations show that formation of the base-on radical anion, step 12 of Scheme 3 (single ET to the corrin ring π^* singly occupied molecular orbital (SOMO)) does not involve significant changes in nuclear coordinates,[30] so λ should be due mainly to the solvent reorganization energy. The work terms result in the usual Frumkin double-layer (DL) electrostatic correction if nonpolar contributions are ignored. Since the Butler−Volmer equation (eq 1) was used to analyze the CV curves, a linearized form of eqs 4 and 5 should be used to give an equation of the form of eq 1, but where the phenomenological parameters k° and α can be expressed in terms of the parameters of the Marcus−Hush theory. Then, $\alpha = 1/2 + [(w_r - w_p)/2\lambda_0]$,[31] with $w_r = zF\phi_2$ and $w_p = (z - 1)F\phi_2$, where ϕ_2 is the DL potential at the reaction plane, taken to be the outer Helmholtz plane (OHP), and z is the charge on the oxidized species, i.e., Me-Cbl. The measured apparent

(30) PM3 geometric optimization on the entire Me-Cbl molecule, which gives accurate nuclear coordinates comparable with those obtained from DFT calculations, indicates that the bond distance change on going to the radical anion is <0.01 Å for Co−C and <0.02−0.04 Å for ring Co−N and Co−N in the DBz.

(31) Kojima, H.; Bard, A. J. *J. Am. Chem. Soc.* **1975**, *97*, 6317. These authors point out that the phenomenological charge-transfer coefficient, expressed in terms of the Marcus parameters, is $\alpha = 1/2 + [\Delta G^{\circ} + (w_r - w_p)/2\lambda_0]$. We have left out ΔG° in this expression so that the $i-V$ expression is truly linearized and α in the Frumkin correction is defined the same way as α in the exponential terms for electrode potential in the Butler−Volmer equation.

standard heterogeneous rate constant, k°, assuming an adiabatic ET, is given in terms of eqs 1 and 3 and linearized versions of eqs 4 and 5 as

$$k^\circ = Z\kappa\, e^{(\alpha n - z)F\varphi_2/RT} \exp(-\lambda_0/4k_BT) \quad (6)$$

To calculate if $\kappa \approx 1$ from the experimental value of k°, we need values for Z, ϕ_2, α, and λ_0. The collision number, expressed in centimeters per second, at an electrode is $Z = 1000(RT/2\pi M)^{1/2}$, where M is molar mass in kilograms per mole (Me-Cbl = 1301 g/mol), giving 1.7×10^3 cm/s. We estimate $\phi_2 = -0.068$ V from data in ref 31 (in pure DMF/electrolyte solution), and the outer or solvent reorganization energy is calculated from the Marcus formulation of the free energy change (solvation) on charging due to a unit charge change on a spherical molecule in a dielectric continuum,

$$\lambda_0 = \frac{{e_0}^2}{4\pi\epsilon_0}\left(\frac{1}{D_{op}} - \frac{1}{D_{st}}\right)\frac{1}{4a} \quad (7)$$

assuming imaging in the electrode, where e_0 is the electron charge, D_{op} and D_{st} are the optical and static dielectric constants of the solvent, respectively, and ϵ_0 is the permittivity of free space. This formulation fits our data better than the Hush formulation, which gives a value twice that given by eq 7. Using an average value for $D_{st} = 34.3$ ($D_{MeOH} = 32.7$, $D_{DMF} = 36.7$), $D_{op} = 2$, at $T = 293$ K and a radius $a = 8.1$ Å (from the diameter of a PM3 structure) for Me-Cbl, a value of 0.209 eV is calculated from eq 7.

Using the parameters $k^\circ = 0.016$ cm/s, $\lambda_0 = 0.21$ eV, $Z = 1.7 \times 10^3$ cm/s, $\phi_2 = -0.068$ V, $z = 0$, $n = 1$, and $\alpha = 0.77$ results in $\kappa = 2.1 \times 10^{-4}$ from eq 6, indicating nonadiabatic ET. The true standard heterogeneous rate constant, k°_{12}, is related to the measured value k° by the relationship $k^\circ_{12} = k^\circ/e^{(\alpha n - z)F\varphi_2/RT}$, and after the correction is 0.13 cm/s at 293 K.

It should be appreciated that the value of k° calculated by simulation is an averaged value of a set of rate constants which vary because of the change in double-layer potential over the region from -1.35 to -1.55 V vs our Ag/AgCl nonaqueous reference electrode. On the basis of the data in ref 31, Savéant[32] has given a relationship $\phi_2 = 0.011E - 0.052$ for DMF solvent and tetrabutylammonium electrolyte. While our mixed solvent is not exactly the same, it is close enough to use this relationship to predict that a change, $\Delta\phi_2$, of only -0.002 V takes place over the simulation potential range, so the variation in ϕ_2 will not be large enough to affect the measured k°. Also, according to the linearized Marcus–Hush theory, the value of the charge-transfer coefficient $\alpha = 0.5 - (e_0\phi_2(\text{eV})/2\lambda_0) = 0.66$ for $z = 0$ and $\phi_2 = -0.068$ V. Although this indicates that α is a function of ϕ_2, it should not change within the two significant figures accuracy over the potential range of the simulation. Furthermore, although this value of $\alpha = 0.66$ is larger than 0.5, it is not equal to the experimental value $\alpha = 0.77$ found in the simulation–curve-fitting, which could mean that the curvature of the free energy curves of reactant and product are not equal, as assumed in the theory.

We can also consider a value of κ calculated using a formulation for the pre-exponential factor Z in terms of an "encounter preequilibrium".[33] In this case, $Z' = \nu_n\delta_r$, where ν_n is a nuclear frequency factor and δ_r is a reaction zone thickness. If we take $\nu_n = 5 \times 10^{13}$ s^{-1} and $\delta_r = 1 \times 10^{-8}$ cm, then $Z = 5 \times 10^4$ cm/s, a typical value found experimentally and from solvent dynamics;[32] however, in our case there may be a steric factor which should lower this value somewhat. Thus, for simplicity, we take $Z' = 1.7 \times 10^4$ cm/s, a factor of 10 times the Z calculated as a collision frequency, which gives $\kappa = 2.1 \times 10^{-5}$ cm/s, again indicating that the ET process is nonadiabatic.

Having established that the ET process is nonadiabatic, we now consider an approximate nonadiabatic rate constant expression with a classical reorganization energy which gives $Z\kappa$ explicitly. According to Marcus,[28] in the nonadiabatic case, κ is the value of the transmission coefficient at the Fermi level. Using the density of states at the Fermi level and assuming that the electronic matrix coupling element, $\langle V\rangle^2$, is independent of energy, Tanaka and Hsu[34] derived an approximate expression for the standard heterogeneous rate constant at metal electrodes by integrating over the filled metal energy level with a step function replacing the Fermi–Dirac distribution expression. For values of $\lambda_0 > k_BT$,

$$k = \frac{6\pi\Delta z N\langle V\rangle^2}{hE_F}\left(\frac{\pi k_BT}{\lambda}\right)^{1/2} \exp\left(-\frac{\lambda}{4k_BT}\right) \quad (8)$$

where h is Planck's constant, N is metal free electron concentration per atom, and E_F is the Fermi energy, and we need to include Δz (in order to get centimeter per second units), which is an effective width at a distance from the electrode surface where the probability of ET is high for a freely diffusing species. Comparing eqs 6 and 8, and using the density of states relationship $\rho(E_F) = 3N/2E_F$, the explicit relationship $Z\kappa = (4\pi\Delta z\rho/h)\langle V\rangle^2(\pi k_BT/\lambda)^{1/2}$ is found. This shows that the pre-exponential term of the standard heterogeneous rate constant should depend on $T^{1/2}$ for this approximation and also allows a calculation of the electronic matrix coupling element. A similar temperature dependency for monolayers has been obtained[35] from Chidsey's formulation of the Marcus relationship and also by Gosavi and Marcus.[36]

We can now use eq 8 to calculate an estimate of the electronic coupling matrix element, $\langle V\rangle^2$, which is the square of the average value of the matrix element $\langle\Psi_k|H_{el}|\Psi_A\rangle = \bar{H}_{kA}$, which expresses the coupling between the metal wave functions Ψ_k and the acceptor orbitals Ψ_A of the redox species (Me-Cbl) involved in ET. The experimentally measured apparent heterogeneous rate constant for ET in terms of the coupling matrix element becomes, for uncharged ($z = 0$) Me-Cbl,

$$k^\circ = 4\pi\Delta z\frac{\rho(E_F)}{h}\langle V\rangle^2\, e^{\alpha F\varphi_2/RT} \exp(-\lambda_0/4k_BT) \quad (9)$$

The value of the density of states can be estimated by assuming that a single Ag atom couples with the molecular state at the Ag amalgam/solution interface. For Ag the free electron concentration[37] is 5.85×10^{22}/cm^3, which, using an atomic

(32) Savéant, J.-M. *J. Am. Chem. Soc.* **1992**, *114*, 10595–10602.
(33) Hupp, J. T.; Weaver, M. J. *J. Electroanal. Chem.* **1983**, *152*, 1–14.
(34) Tanaka, S.; Hsu, C.-P. *J. Chem. Phys.* **1999**, *111*, 11117–11134.
(35) Smalley, J. F.; Feldberg, S. W.; Chidsey, C. E. D.; Linford, M. R.; Newton, M. D.; Liu, Y.-P. *J. Phys. Chem.* **1995**, *99*, 13141–13149.
(36) Gosavi, S.; Marcus, R. A. *J. Phys. Chem. B* **2000**, *104*, 2067–2072.
(37) Kittel, C. *Introduction to Solid State Physics*, 6th ed.; Wiley: New York, 1986.

radius of 1.52 Å to calculate atomic volume, gives $N = 0.88$/atom. The Fermi energy,[37] E_F, is 5.48 eV/atom, so $\rho(E_F) = 3N/2E_F = 0.24$ states/eV. This value of density of states is similar to those used for Au (0.27[38] and 0.29[36]) in the literature, and the value for Hg based on the free electron model should not be too different since Ag, Hg, and Au are s-band metals having similar Fermi energy and atomic volume. Using reasonable values of $\Delta z = 1.0 \times 10^{-8}$ cm, $\lambda_0 = 0.21 \pm 0.05$ eV, $\phi_2 = -0.068 \pm 0.005$ V, $\rho(E_F) = 0.24 \pm 0.03$ states/eV, and $k^\circ = 0.016 \pm 0.001$ cm/s, a value of $\langle V \rangle^2 = (2.2 \pm 0.8) \times 10^{-7}$ eV^2, or $\bar{H}_{kA} = (4.7 \pm 1.1) \times 10^{-4}$ eV (~46 J/mol), is calculated from eq 9 at $T = 293$ K. Here, the uncertainty in λ_0 dominates the propagation of errors and leads to a 59% uncertainty in the result. Even with this magnitude of error, we can say for certain that the value of $\langle V \rangle^2$ is in the range of a nonadiabatic ET at the stronger end of the weak electron coupling regime. This value of $\bar{H}_{kA}$ is around 100 times larger than those measured for ET through osmium-containing monolayers on Ag and Hg electrodes.[39]

Estimation of the Thermodynamic Reduction Potentials for Other Alkylcobalamins. In simulations using the previously determined $E^{\circ\prime}$, k°, and α values of Me-Cbl, the CV is found to be totally irreversible at 0.3 V s^{-1} as the rate of the reaction becomes faster than 1×10^4 s^{-1} (Figure S3). This simulation shows that if the reaction rate is changed from 1×10^4 to 1×10^5 s^{-1}, the peak potential is only shifted positive by 2 mV. Thus, the simulation−fitting of a CV would not give any data on chemical bond-breaking rate constants for ethylcobalamin, *n*-propylcobalamin, *n*-butylcobalamin, 2-butylcobalamin, and adenosylcobalamin, which have reaction rates much faster than the 5.50×10^3 s^{-1} value of Me-Cbl. On the other hand, we can use the fact that the reaction rate will not affect the peak potential to calculate a formal reduction potential from the CV curves. In a scan rate region less than 2 V/s, all of the alkylcobalamins show a similar irreversible shape in the cyclic voltammetry. However, their peak potentials are strongly influenced by the alkyl substituent (Figure 2). We assume they will all follow the detailed electrode process depicted in Scheme 3, which means that, at low scan rates, they can all be simulated by a quasi-reversible electrode process with a single fast subsequent reaction.

It is clear that, at a scan rate of 0.3 V/s, the electrode process with the fast subsequent step is in the intermediate kinetic (KI) zone of the zone diagram for the EC mechanism[40] with a quasi-reversible electrode process (log $\Lambda = 0.28$, log $\lambda = 2.93$). It turns out that all of the alkylcobalamins are all very similar in shape and slope at the foot of the CV curve, and thus all of the alkylcobalamins should have very similar values for the rate constant of the ET step, k°_{12}. We give results in the electronic structure section which are consistent with this assumption. Thus, using a rate constant of 1×10^4 s^{-1} and the k° of Me-Cbl, we determine the formal reductions potentials of the other alkycobalamins through simulation and curve-fitting. The estimations of the potentials determined in this way are as follow (in volts): methylcobalamin, −1.47; ethylcobalamin, −1.35; *n*-propylcobalamin, −1.35; *n*-butylcobalamin, −1.37; 2-butylcobalamin, −1.32; and adenosylcobalamin, −1.31 (all vs a nonaqueous Ag/AgCl reference electrode; Table 2).

Table 2. Comparison of Electrode Potentials with Electronic Structure Parameters of DFT Geometry-Optimized Data for Alkylcobalamins (Model 1) Compared with the Negative of the Measured Formal Redox Potential, $-E^\circ_{12}$[a]

	methyl	*n*-butyl	ethyl	*n*-propyl	2-butyl	2-propyl
$-E^\circ$	1.47	1.37	1.35	1.35	1.32	1.30[b]
$R_{Co(III)-C}$	1.988	2.024	2.024	2.024	2.084	2.076
$R_{Co(III)-C}$, PM3 semiempirical	1.978	2.020	2.019	2.021	2.060	2.059
$R_{Co(II)-C}$	1.980	2.017	2.011	2.014	2.050	2.050
$R_{Co(III)-N}$	2.197	2.222	2.223	2.225	2.239	2.247
$R_{Co(II)-N}$	2.202	2.205	2.233	2.212	2.260	2.261
U_{LUMO}	−4.84	−4.82	−4.83	−4.83	−4.75	−4.77
U_{SOMO}	−2.61	−2.64	−2.63	−2.63	−2.62	−2.62
U_{diss}	4.51	4.28	4.25	4.27	3.89	3.91

[a] R_{Co-C} and R_{Co-N}, axial Co−C and axial Co−N3 bond distances of the cobalamin base-on model in angstroms; U_{LUMO}, LUMO energy of the R-Co(III)Cbl base-on model in electronvolts; U_{SOMO}, SOMO Energy of the R-Co(II)Cbl base-on model in electronvolts; U_{diss}, difference in total energy (eV) for the reaction R-Co(III)$Cbl_{base-on}$ = Co(I)Cbl + DBz +R. [b] This potential comes from the data in ref 19.

The values of α determined for all tested alkylcobalamins were found to be larger than 0.5, indicating that the structure of the transition state for reduction is close to that of the reactant.[26] Lower values of α were found for isobutylcobalamin and adenosylcobalamin, suggesting that their structures in the transition state have less similarity to the reactant than methyl-, ethyl-, and *n*-propylcobalamins.

The estimated formal reduction potentials of the alkylcobalamins show an interesting grouping. Methylcobalamin has the most negative formal reduction potential. Ethylcobalamin, *n*-propylcobalamin, and *n*-butylcobalamin have more positive values, but their formal reduction potentials are quite close together. The $E^{\circ\prime}$ shift of 117 mV from methylcobalamin to ethylcobalamin is larger than could be expected for a base-on/base-off effect. A similar shift of 70 mV, obtained by linear scan voltammetry, was reported in DMF.[19] According to results of typical linear free energy plots for polarographic half-wave potentials,[41] an electron-donor substituent shifts the formal reduction potential negatively. From methyl to ethyl, *n*-propyl, *n*-butyl, and isobutyl, the alkyl electron-donor property is increased, which should favor the $E^{\circ\prime}$ shift negatively in theory; however, we find that the $E^{\circ\prime}$ values are shifting positively as the alkyl group becomes more branched.

Without a detailed analysis of the electrode process, but by a thermodynamic argument using the potential of the Cbl(II)/Cbl(I)$^-$ couple and an estimation of the free energy of bond breaking, it was suggested by Zhou, Tinembart, Scheffold, and Walder[19] that the peak potentials are related to a reduction process involving bond breaking. Peak potential shifts were interpreted in terms of a bond-energy decrease due to steric hindrance in the ground state. Furthermore, these authors suggested that the measured peak potentials were close to thermodynamic potentials. The nonbonding interactions between the alkyl group and the corrin ring side chains were indicated as the cause of the potential shifts since a similar shift with alkyl substituent is not observed for non-cobalamin B_{12} model cobalt complexes.[19] We will explore the relationship between

(38) Royea, W. J.; Fajardo, A. M.; Lewis, N. S. *J. Phys. Chem. B* **1997**, *101*, 11152−11159.
(39) Forster, R. J.; Loughman, P.; Keyes, T. E. *J. Am. Chem. Soc.* **2000**, *122*, 11948−11955.
(40) Nadio, L.; Savéant, J. M. *J. Electroanal. Chem.* **1973**, *48*, 113−145.
(41) Zuman, P. *Substituent Effects in Organic Polarography*; Plenum: New York, 1967.

the measured formal potentials of the alkylcobalamins compounds and their molecular parameters as calculated by electronic structure calculations in the next section.

Electronic Structure Calculations. We have made DFT electronic structure calculations on the alkylcobalamins for all of the alkyl substituents which were studied electrochemically. The model of R-Cbl(III) that we used includes the full corrin ring with all side-chain groups replaced by hydrogen atoms and with the dimethylbenzimidazole base ligand replaced by benzimidazole, as shown in model 1.

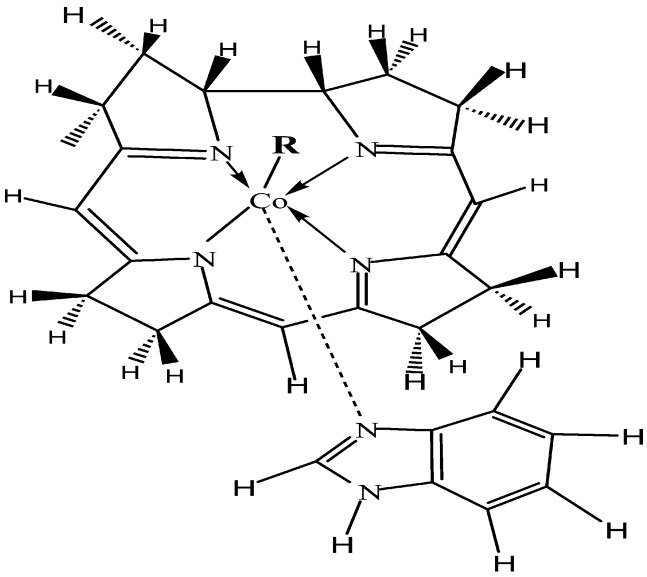

Model 1

Since the model does not include the negative phosphate-containing side chain, the R-Cbl(III) model is a singly plus charged species. The calculations were made with the Gaussian 03 package of programs using the B3LYP hybrid functional level of theory and the LANL2DZ double-ζ basis set. This basis set was used for all atoms and contains the relativistic effective core potential for the cobalt atom. All geometric optimizations were made to the default tolerances of Gaussian. Although similar DFT calculations have been made[17,42−46] for R-Cbl(III) compounds, they had not been done for some of our R substituents, and so we did the calculations for all of our alkyl groups. There has been some concern about the B3LYP hybrid functional giving Co−C dissociation energies which are too low, but these[46] were compared to earlier experimental results (our experimental results are nominally 6 kcal mol^{-1} lower than the previous ones); however, more importantly, the chemical models are not good enough to invalidate this functional. Also, there have been no calculations for the one-electron-reduced products, the R-Cbl(II) species. Actually, these reduced species do not appear to have much Co(II) character since the SOMO for the doublet species is mostly a corrin ring π^* MO with only a little

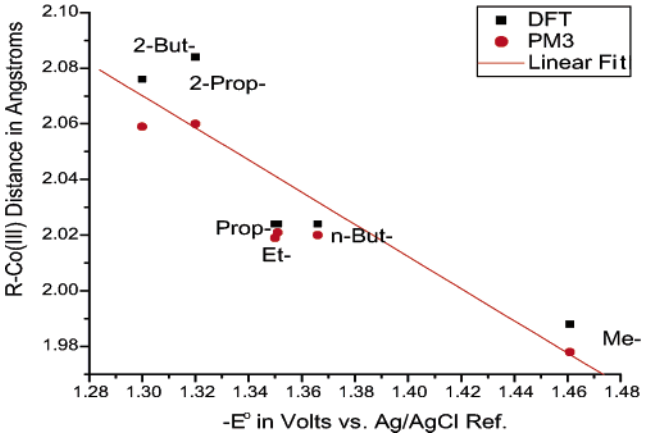

Figure 8. Plot of C−Co bond distance (Å) from electronic structure calculations vs experimentally estimated thermodynamic reduction potentials. Squares are calculated by B3LYP/LANL2DZ on R-corrin-benzimidazole model 1 compounds, and circles with PM3 on the complete R-cobalamin molecules.

d_{yz} character. The results for the bond distances and total energy calculations are given in Table 2.

We have also included in Table 2 Co(III)−C bond distance data calculated for the entire R-cobalamin molecule with all side chains using the semiempirical PM3 method of the Spartan04 program. The PM3 and DFT bond distances, $R_{Co(III)-C}$, are very close, i.e., within 0.005 Å except for 2-butyl and 2-propyl, where the difference is slightly larger. A plot of $R_{Co(III)-C}$ versus the estimated reduction potentials (Figure 8) has a straight line fit with a linear correlation coefficient of 0.89.

From Figure 8, showing $R_{Co(III)-C}$ distances vs $E°_{12}$, we see the points group together in terms of the nature of the alkyl group. Thus, Me-Cbl(III) is separated from the rest, having the shortest bond distance; the ethyl-Cbl(III), *n*-propyl-Cbl(III), and *n*-butyl-Cbl(III) have nearly the same values and are about 0.03−0.04 Å longer than Me-Cbl(III); and the branched alkyls, 2-propyl and 2-butyl, have the largest $R_{Co(III)-C}$, 0.04−0.06 Å longer than for the normal alkylcobalamins. Therefore, as the calculated Co(III)−C distance gets longer, the potential moves to more positive values. We have not included deoxyadenosylcobalamin in this plot since its behavior is quite different. Our calculation of its PM3 Co−C bond distance is 2.021 Å,[47] which is closest to those for the straight-chain alkyl groups, but its reduction potential according to our measurement is −1.31 V, which is similar to those for the molecules with branched alkyl groups. This indicates that its effect on the potential is more complicated than that of the simple alkyl groups and involves the entire deoxyadenosyl group.

What is clear for the alkylcobalamins in the plot is that the potential scales with the Co−R bond distance, and thus it is scaling with bond energy, as is shown by the data in last row in Table 2. This row gives the calculated total energy difference, U_{diss}, for the vacuum reaction, R-Co(III)model$_{base-on}$ = Co(I)-model + Bz + R, which is a reductive dissociation process in which the parent six-coordinate R-Co(III) base-on model is dissociated to the four-coordinate Co(I) model as the benzimidazole base and alkyl radical come off. A plot of U_{diss} vs the electrode potential exactly mirrors the bond distance vs electrode

(42) Jensen, K. P.; Sauer, S. P. A.; Liljefors, T.; Norrby, P.-O. *Organometallics* **2001**, *20*, 550−556.
(43) Andruniow, T.; Zgierski, M. Z.; Kozlowsky, P. M. *J. Am. Chem. Soc.* **2001**, *123*, 2679−2680.
(44) Dölker, N.; Maseras, F.; Lledos, A. *J. Phys. Chem. B* **2001**, *105*, 7564−7571.
(45) Dölker, N.; Maseras, F.; Lledos, A. *J. Phys. Chem. B* **2003**, *107*, 306−315.
(46) Jensen, K. P.; Ryde, U. *J. Phys. Chem. A* **2003**, *107*, 7539.

(47) A DFT calculation for a model 1 structure with R = 5′-deoxy-5′-adenosyl but with dimethylbenzimidazole as the base gives 1.992 Å as the Co−C bond distance.[43]

potential plot, with the points clustered the same way and with the same linear correlation coefficient, 0.89. This shows that the measured electrode potential for reduction to the radical anion is directly related to the bond dissociation energy, which means the LUMO or SOMO energies should also be influenced by the alkyl group, i.e., the bond energies. However, the values of U_{HOMO} and U_{SOMO} in Table 2 do not show much change with alkyl group! These facts show that the ground-state calculations for the orbital energies of the LUMO of R-Cbl or the SOMO of the radical anion do not correlate with their measured one-electron reduction potentials or R−Co bond lengths, and we suggest that a calculation based on a better model involving vibronic coupling is needed to show this correlation.

Table 2 also shows that the calculated bond distances for the Co−C bond in our model alkyl compounds do not change significantly when one electron is added to the model compounds. Also, the Co−N bond distance from the N3 (ϵ-nitrogen) of the axial benzimidazole does not change greatly on reduction; compare $R_{Co(III)-N}$ and $R_{Co(II)-N}$ in Table 2. We have also found small changes in internal coordinates using PM3 calculations on the entire Me-Cbl molecule[30] and interpreted all these results as indicating that there is very little inner reorganization energy in the reduction process. Both the DFT and the PM3 methods are known to give structures that agree well with X-ray structural data for Me-Cbl. However, one would expect some difference in order to correlate with the reduction potential shifts. Again it would appear that a "single-configurational" DFT calculation is not completely adequate and a multireference, multiconfigurational approach is necessary to correlate energy shifts with alkyl group.

Figure S4 in the Supporting Information shows the energy levels around the highest occupied molecular orbital (HOMO), the LUMO, and the σ* Co−C MO from the single-configurational DFT calculations for the model base-on Me-Cbl(III)$^+$, for the one-electron-reduced base-on and base-off model Me-Cbl species, and for the model Cbl(I). The difference between the bonding and antibonding Co−C σ MOs in the model Me-Cbl$^+$ is 5.00 eV, and the HOMO-to-LUMO gap is 3.1 eV. The difference in energy between the π* SOMO and the σ* Co−C MO is just as large, if not larger than 5 eV in the one-electron-reduced base-on species (here the σ* energy is not shown, since it is above the 0.0 eV level); however, it is lowered to 2.15 eV in the one-electron-reduced base-off species. With the electron excited into the σ* orbital, a time-dependent DFT calculation gives this energy difference as 1.4 eV for the base-off species, which suggests there can be strong vibronic coupling of the orbitals. These energy differences between the π* SOMO and σ* Co−C MOs imply that the dissociative ET mechanism should go through the base-off radical anion, as in Scheme 3. In fact, ground-state DFT calculations which we have made for the potential energy of radical anion (model 1) as the C−Co bond is stretched show that the dissociation energy is 0.5 eV lower for the base-off than for the base-on species.

The estimation of the reduction potentials from the CV data involves the assumption that the heterogeneous rate constant for ET does not change substantially with alkyl group. This assumption implies that the matrix coupling element and the outer reorganization energy do not change significantly with alkyl substituent. The outer reorganization energy in the Marcus model is dependent on the radius of the molecule. The molecular volumes of the alkylcobalamins as calculated by the PM3 method are all very close to that of methylcobalamin (within 2.4%), with only *n*-butylcobalamin being about 4% larger. Considering that the electronic structures of the alkylcobalamins are similar as well as their volumes, the assumption that their heterogeneous rate constants should be very close seems reasonable. This also means that their solvation energies should not be too different, although these were not included in the calculations summarized in Table 2.

Bond Energies and Rate-Determining Step. The electrode potential measured from the CV is for the one-electron reduction to the radical anion. We can add to this potential the necessary thermodynamic potentials for reduction to the solvent-separated products of Scheme 3. To obtain this potential, $E^{\circ\prime}_{16} = E^\circ$ (R-Cbl(III)/Cbl(I)$^-$ + R$^\bullet$), requires equilibrium constants K_{23}, K_{35}, and K_{56} for the additional steps in the reduction of Me-Cbl. The additional potential at 20 °C is 0.0581 log($K_{23}K_{35}K_{56}$). K_{56}, which is for the dissociation of the caged species, (Cbl(I)$^-$ + R$^\bullet$)$_{cage}$ = R$^\bullet_{(sol)}$ + Cbl(I)$^-_{(sol)}$, is estimated as $K_{56} = 0.77$.[48] We estimate that $K_{25} = K_{23}K_{35}$ is between 0.01 and 2.0 at 293 K using Figure S1 and the fast scan data. Thus, $E^{\circ\prime}_{16} = -1.47 + 0.0581 \log(K_{23}K_{35}K_{56})$ will be between −1.45 and −1.59 V vs our nonaqueous Ag/AgCl reference. The free energy for this potential is thermodynamically equivalent to the sum of the free energy of the Me-Cbl bond-breaking reaction (base-on to base-on) and the free energy of reduction potential of the Cbl(II)/Cbl(I)$^-$ (base-on to base-off) couple,

$$\text{R-Cbl(III)}_{(sol)} = \text{Cbl(II)}_{(sol)} + \text{R}^\bullet_{(sol)}, \quad \Delta G^\circ_{diss}$$

$$\text{e}^- + \text{Cbl(II)}_{(sol)} = \text{Cbl(I)}^-_{(sol)}, \quad \Delta G^\circ_{12r/12s}$$

This summation gives the relationship

$$E^{\circ\prime}_{16} = -D_{\text{R-Cbl(III)}} + T(\bar{S}_R + \bar{S}_{\text{Cbl(II)}} - \bar{S}_{\text{R-Cbl(III)}}) + E^{\circ\prime}_{B_{12r}/B_{12s}} \quad (10)$$

where D_{diss} is the bond dissociation enthalpy (BDE) of R-Cbl(III), $\bar{S}_i$ are partial molar entropies of the indicated species, and the electrode potentials must be converted to proper energy units. We can use the above relationship to estimate D_{diss} for Me-Cbl at 293 K from this thermodynamic cycle. We have the range $E^{\circ\prime}_{16} = -1.45$ to -1.59 V vs the nonaqueous reference electrode from the above estimates and $E^{\circ\prime}_{12r/12s} = -0.75$ V vs the nonaqueous reference electrode.[49] In addition, in order to get a value for D_{diss}, we need to estimate $T\Delta S$. We estimate ΔS by assuming that the partial molar entropies of R-Cbl(III) and Cbl(II) are close and cancel, so $\Delta S = S^\circ\{R\}_{(sol)}$. The value of $S^\circ\{CH_3\}$ we use is 46.4 cal K^{-1} mol^{-1}.[50] Taking

(48) This value is calculated for the formation of a cage, A + B = [AB]$_{cage}$, where A and B have no interaction, with $\Delta G^\circ_{cage} = -RT \ln(K)$, where $K = (4/3)\pi(R_A + R_B)^3$ is the volume in liters per mole of a spherical model of the encounter pair per unit volume (dimensionless) (Moore, J. W.; Pearson, R. G. *Kinetics and Mechanisms: A Study of Homogeneous Chemical Reactions*; John Wiley & Sons: New York, 1981; p 240). The PM3 molecular volume of the base-off radical anion of Me-Cbl is 1253 Å^3; however, because of the amide side chains, the molecular volume does not change when the methyl radical comes off. The radius of the planar methyl radical is 1.07 Å, so the encounter complex should have a radius of about $R_A + R_B = 8$ Å, or $V = 2.1 \times 10^3$ Å^3; then $K = 1.3$ and $K_{56} = 1/K = 0.77$.

(49) This value was measured at ambient temperature from the CV of aquocobalamin (0.50 mM in 0.2 M TBAF) on a Hg drop from the average of the cathodic and anodic peak potentials in DMF and methanol (40:60) at a scan rate of 5 mV/s.

$T\Delta S = (293)(46.5) = 13.6$ kcal/mol, a D_{diss} between 30 and 33 kcal/mol is calculated for the thermodynamic BDE from the spread in the product of stepwise equilibrium constants. The estimated error in ΔS (± 5 eu or 1.5 kcal/mol) is smaller than the spread in the $\log(K_{23}K_{35}K_{56})$ contribution, so we set BDE $= 31 \pm 2$ kcal/mol. It should be noted that the kinetic data give $D_{thermolysis} = 37 \pm 3$ kcal/mol and $\Delta S_{thermolysis} = 24 \pm 6$ cal K^{-1} mol $^{-1}$.[6] Here, $D_{thermolysis}$ is calculated by subtracting the viscous flow activation enthalpy in ethylene glycol solvent (reverse activation enthalpy) from the observed solution activation enthalpy (forward activation enthalpy) to get a thermodynamic BDE.[6,51] Our value is certainly less than that found by kinetic studies of Me-Cbl(III) thermolysis; however, considering that solvents are different and that differential solvent effects would have to be considered to get a gas-phase BDE, the two values probably represent nearly the same gas-phase BDE within the range of experimental errors and the different solvent effects.

As already discussed, a similar but more approximate calculation was made by Zhou et al.[19] to suggest that peak potentials for alkylcobalamin reduction contain information on BDEs, and they used $\Delta S = 50$ eu in their calculation. Unfortunately, the BDEs of the other alkylcobalamins cannot be calculated from the electrode potentials because it is critical to have more accurate entropies for the other R-Cbl(III) and the Cbl(II) species in order to use the known entropies of the alkyl radicals.

The steps in Scheme 3 which follow the initial ET involve the dissociation of the axial dimethylbenzimidazole base followed by the homolytic C−Co bond breaking; the latter can be thought of as intramolecular ET, as suggested by Savéant[12d] in his dissociative electron-transfer theory. We can estimate the BDE of this base-off radical anion, D_{RX^-}, from the expression $D_{RX^-} = \Delta G_{RX^-} + T(S_{Me} + S_{Cbl^-} - S_{Me-Cbl})$. This gives $D_{RX^-} = 13$ kcal/mol for the process to form the solvent-separated R$^\bullet$ (methyl radical) and X^- (Cbl(I)$^-$),[52] assuming the cage dissociation free energy is negligible. This value suggests that the BDE of the base-off radical anion is less than half the BDE of the parent Me-Cbl. This was first pointed out by Finke and Martin,[6] who estimated this BDE as 12 kcal/mol on the basis of the temperature dependence of the homogeneous rate constant of Me-Cbi found in the study by Lexa and Savéant.[2]

The above BDE value should lead to a very fast bond cleavage reaction according to Savéant's theory of dissociative ET.[12d] The activation energy, ΔG^*_{cleav}, given by this theory for the intramolecular dissociative (homolytic) ET step is

$$\Delta G^*_{cleav} = \left(\frac{(\sqrt{D_{RX^-}} - \sqrt{D_{R\cdot\cdot X^-}})^2 + \lambda_0}{4}\right) \times \left(1 + \frac{E^\circ_{(RX/RX^-)} - E^\circ_{RX/(R,X^-)}}{(\sqrt{D_{RX^-}} - \sqrt{D_{R\cdot\cdot X^-}})^2 + \lambda_0}\right)^2 \quad (11)$$

where D_{RX^-} is the BDE for the base-off radical anion, $D_{R\cdot\cdot X^-}$ is the attractive interaction between the caged ion and radical,[18] λ_0 is the reorganization energy in the intramolecular ET step, and the E° values are estimated for the steps as $E^\circ_{13} = -1.43$ V and $E^\circ_{15} = -1.55$ V; all units can be in eV. Since the cobalamin part of the molecule contains the negative charge of the added electron in the radical anion, there should not be much of a change in outer reorganization when the bond breaking occurs; thus, λ_0 is taken as negligible with respect to BDEs. Taking our value $D_{RX^-} = 13$ kcal/mol or 0.57 eV, and using $D_{R\cdot\cdot X^-} = 2$ kcal/mol or 0.09 eV, gives $\Delta G^*_{cleav} = 0.12$ eV or 3.0 kcal/mol from eq 11. This activation energy for the bond breaking gives a rate constant $k_{35} = Z\exp(-\Delta G^*_{cleav}/RT)$. We estimate the unimolecular frequency factor Z for the dissociation of the Me-Cbl radical anion by using $Z = 1 \times 10^{11}$ s^{-1}, which was used for the dissociation of aryl halide radical anions in 1-methyl-2-pyrrolidinone solvent at 293 K.[13] Using this value and estimating the effect of a first power dependence on temperature gives $Z = 8 \times 10^{10}$ at $T = 243$ K. Compared to the latter, the experimental value from Figure 4 of $Z = 0.97 \times 10^9$ at $T = 243$ K in the 40:60 DMF/MeOH solvent is about 100 times smaller; however, this smaller value for the pre-exponential factor refers to the rate-determining step, which is not necessarily the cleavage step. Thus, we take a higher Z value of 5×10^{10} as reasonable for the bond-breaking step and get $k_{35} = 2 \times 10^8$ s^{-1} using the above Savéant theory of dissociative ET. If the ion−radical interaction is entirely negligible, a value of $k_{35} = 4 \times 10^6$ s^{-1} results. In either case, this rate constant is much higher than the measured overall rate constant but is consistent with the results from the model, where this rate is for step 35, which is assumed to be fast in the steady-state process, and step 56 is the rate-determining step.

In Scheme 3 we show the irreversible step as the release of the fragments from the solvent cage, but this is oversimplified. It is likely that this step is an equilibrium step, followed by irreversible solvent attack on the methyl radical as in Scheme 2.[6] Similar to Koenig and Finke,[51,53] we can expand the reaction with an additional trapping step as shown in Scheme 4, where the trapping agent, T, comes from the DMF/MeOH solvent mixture. If all the forward and backward reactions are fast following the ET step and a steady-state condition can be made for the separated Me radical and Cbl(I)$^-$ ion, then the overall homogeneous (chemical) irreversible rate constant measured by fast-scan CV and our DPSC experiment is $k_{chem} = K_{23}K_{35}(k_{56}k_T)/(k_{-56} + k_T)$, where the trapping rate constant $k_T = (k_{T1} + k_{T2})$ is a sum of pseudo-first-order constants, with each second-order rate constant multiplied by the solvent concentration of either DMF or MeOH. If the rate constant for cage re-formation is larger than the rate constant for H abstraction, i.e., $k_{-56} \gg k_T$, then trapping is the rate-determining step. Under these conditions, $k_{chem} = K_{23}K_{35}K_{56}k_T$, where $K_{56} = k_{56}/k_{-56}$. On the other hand, if the reverse is true and $k_T \gg k_{-56}$, then the rate-determining step is the breaking out of the cage to form separated solvated radical and ion, and $k_{chem} = K_{23}K_{35}k_{56}$. This is also the case if the trapping reaction is a rapid reaction of the radical with Hg from the electrode material.[54]

If the former case were true and the solvent controlled the trapping reaction, then the observed k_{chem} should increase if the

(50) The value $S^\circ\{CH_3\}_{(g)} = 46.5$ cal deg^{-1} mol^{-1} has been reported: Hush, N. S. *Z. Electrochem.* **1957**, 734−738. A value $S^\circ_{300}\{CH_3\} = 46.4$ cal deg^{-1} mol^{-1} has been used for bond dissociation enthalpy calculations in isooctane solution: Castelhano, A. L.; Griller, D. *J. Am. Chem. Soc.* **1982**, *104*, 3655−3659.

(51) Koenig, T. W.; Hay, B. P.; Finke, R. G. *Polyhedron* **1988**, *7*, 1499−1516.

(52) $K_{35} = 0.1$ gives a value of 1.3 kcal/mol for the free energy of dissociation of the base-off radial anion, ΔG_{RX^-}, i.e., for reaction of [Me-Cbl]$^-$ to the caged species. The entropy change in the reaction [Me-Cbl]$^- \rightarrow$ Cbl(I)$^-$ + Me$^\bullet$ is found by assuming that Cbl moieties cancel out and using 46.4 eu for the methyl radical.

(53) Koenig, T.; Finke, R. G. *J. Am. Chem. Soc.* **1988**, *110*, 2657−2658.

(54) Lexa, D.; Savéant, J.-M. *Acc. Chem. Res.* **1983**, *16*, 235−243.

Scheme 4

$$\{\text{Me-Cbl}^-\} \underset{}{\overset{K_{35}}{\rightleftharpoons}} \{\text{Me} \cdot\cdot \text{Cbl}^-\}_{cage} \underset{k_{-56}}{\overset{k_{56}}{\rightleftharpoons}} \text{Me}_{(solv)} + \text{Cbl(I)}^-_{(solv)} \xrightarrow{k_T} \text{trapped product}$$

concentration of the more effective H donor is increased, but the opposite seems to occur. That is, when we changed the solvent ratio to one with a higher content of methanol, the rate constant increased, but DMF appears to be a better H donor than MeOH.[55] Thus, the effect of solvent ratio on the overall rate constant of the reaction appears not to be connected with the trapping step but is more likely a dielectric effect or a solvation effect on an earlier step in the mechanism. We therefore suggest that the rate-determining step is the radical and ion separation from the cage, and then $k_{chem} = K_{23}K_{35}k_{56}$.

The Elementary Bond-Breaking Step. It would be useful to know the mechanism whereby the electron in the bound electronic state of the radical anion SOMO π^* orbital goes into the Co−C σ^* antibonding orbital dissociated state with small enough energy difference to allow the fast bond breaking to occur. One possibility is that there is a metastable ground state, S_0^*, which is not represented by the geometrically optimized low-spin structures.[56] It has been suggested that there is a state involving a tautomeric form of the corrin ring which may have very different energetics than the stable ground state.[57] It was proposed that this metastable state could be formed by excited-state decay of a twisted intramolecular charge-transfer (TICT) state. Such a state might be formed thermally in the initial ET process by vibrational activation. Hysteresis observed in redox cycling of corrinoids has been interpreted by Pratt and co-workers[56] in terms of conformational changes in the corrin ring. However, it is still likely that this ground state will be an antibonding π^* radical anion. We have seen that the single-configuration ground-state DFT calculations show that there is a large energy separation between the SOMO π^* level and the σ^* level of the Co−C bond. The semiclassical theory of Savéant indicates that this gap should be much smaller for the intramolecular ET to give the fast kinetics that is observed. Thus, it appears that the bond-breaking process must involve a coupling between the σ^* dissociative state and the bound π^* state. These electronic states are uncoupled by nature of their symmetry, but a coupling can occur by a symmetry-breaking coordinate.

One mechanism which will allow this coupling is the avoided crossing at a conical intersection (CI). This type of mechanism for thermal ground-state reactions has only recently been discussed for species produced by one-electron reduction in solution. Thus, the fragmentation following ET of an aryl-Cl radical anion[58] to give an aryl radical and chloride ion, and the fragmentation of *N*-methoxypyridyl radicals (N−O bond cleavage) to give pyridine-containing compounds and a methoxy radical,[59] have been treated as an avoided crossing at a CI. In the bond cleavage processes of aryl halides, a bending coordinate for motion of the equatorial bond out of the plane of the aromatic ring allows a coupling of the π^* orbital with σ^* orbitals. Such bending can give rise to a mixing of the π^*/σ^* orbitals and provide a reaction path where a CI involving the bond-breaking coordinate and the bending coordinate is avoided, leading to an avoided crossing so that the reaction occurs on the lower adiabatic potential energy surface. This process has also been treated in terms of the theory of intramolecular dissociative electron transfer.[60] It is tempting to invoke such a process in the case of the Me-Cbl radical anion. Here, the bending of the Co−C bond with respect to the plane of the four pyrrole nitrogens, which provide the equatorial coordination of the cobalt in the corrin ring, might also be invoked as a symmetry-breaking coordinate as the Co−C bond stretches. However, this wagging motion may be constrained by side chains of the corrin ring.

An additional possibility for activating symmetry-forbidden intramolecular electron transfer is by vibronic interactions which couple electronic states through symmetry-breaking inner-sphere nuclear vibrations.[61] This type of coupling or some other vibration involving a CI needs to be established by calculations, but whatever the mechanism, it must allow the π^*/σ^* mixing in order to lower the energy of the intramolecular ET process of step 35.

Conclusion

The investigation of the details of the electrochemical cleavage reaction of methylcobalamin shows that it is a stepwise dissociative ET process with a one-electron heterogeneous ET step to form the radical anion, followed by a series of homogeneous reactions. The mechanism cannot be either a concerted bond breaking to directly form solvent-separated products on charge transfer or even a sticky concerted mechanism with a cage species, since the base-on radical anion is a true intermediate, as suggested by the fast-scan CV curves. However, the mechanism of Me-Cbl reductive cleavage we have proposed still involves the cage species. The simulation−curve-fitting allows the measurement of the heterogeneous rate constant for the elementary electrode charge-transfer reaction, which turns out to be a nonadiabatic process. The value of the electronic coupling matrix element shows that the coupling energy is only 1−2 orders of magnitude smaller than the energy of adiabatic electron coupling between the metal surface atoms and the Me-Cbl molecule. The effect of varying the solvent mixture of DMF/MeOH allows us to conclude that the rate-determining step that follows ET is the formation of the solvent-

(55) Andrieux, C. P.; Badoz-Lambling, J.; Combellas, C.; Lacome, D.; Savéant, J.-M.; Thiébault, A.; Zann, D. *J. Am. Chem. Soc.* **1987**, *109*, 1518−1525.
(56) Chemaly, S. M.; Jack, L. A.; Yellowless, L. J.; Harper, P. L. S.; Heeg, B.; Pratt, J. M. *Dalton Trans.* **2004**, 2125−2134.
(57) Pratt, J. M. In *Chemistry and Biochemistry of B_{12}*; Banerjee, R., Ed.; John Wiley & Sons: New York, 1999; p 156.
(58) (a) Laage, D.; Burghardt, I.; Sommerfeld, T.; Hynes, J. T. *J. Phys. Chem. A* **2003**, *107*, 11271−11291. (b) Burghardt, I.; Laage, D.; Hynes, J. T. *J. Phys. Chem. A* **2003**, *107*, 11292−11306. (c) Laage, D.; Burghardt, I.; Sommerfeld, T.; Hynes, J. T. *ChemPhysChem* **2003**, *4*, 61−66.
(59) (a) Lorance, E. D.; Kramer, W. H.; Gould, I. R. *J. Am. Chem. Soc.* **2002**, *124*, 15225−15238. (b) Lorance, E. D.; Kramer, W. H.; Gould, I. R. *J. Am. Chem. Soc.* **2004**, *126*, 14071−14078. (c) Lorance, E. D.; Gould, I. R. *J. Phys. Chem. A* **2005**, *109*, 2912−2919.
(60) Costentin, C.; Robert, M.; Savéant, J.-M. *J. Am. Chem. Soc.* **2004**, *126*, 16051−16057.
(61) (a) Lockwood, D. M.; Ratner, M. A.; Kosloff, R. *J. Chem. Phys.* **2002**, *117*, 10125−10132. (b) Jones, G. A.; Paddon-Row, M. N.; Carpenter, B. K.; Piotrowiak, P. *J. Phys. Chem. A* **2002**, *106*, 5011−5021 (c) Skourtis, S. S.; Waldeck, D. H.; Bratan, D. N. *J. Phys. Chem. B* **2004**, *108*, 15511−15518.

separated methyl radical and cob(I)alamin anion. The overall free energy for the reduction of Me-Cbl to these solvent-separated species gives a CH_3-Co bond dissociation enthalpy of 31 kcal/mol, which is about 6 kcal/mol lower than the previous value found from kinetic studies.

We could not investigate the details of the mechanism of the other alkylcobalamins because the irreversible step is too fast to measure. However, a measurement of the redox potential for the series of alkylcobalamins was correlated with the Co−C bond distance of the various alkyl groups, as found by DFT electronic structure calculations. These calculations also indicate that the elementary bond-breaking step should involve a coupling of the π^* bound state and the σ^* dissociative state of the Me-Cbl radical anion to allow the fast intramolecular charge transfer. Our "single-configurational" DFT calculations for a simplified molecular model do not show a small enough π^*-to-σ^* energy gap, but they do show that the gap is smaller for the base-off reduced species, suggesting that it is involved in a lower energy pathway. Incorporation of conical intersection and/or vibronic effects in the calculation model would be needed to show the required energetics.

The relevance of the electrochemical reductive cleavage mechanism of Me-Cbl to the transfer of a methyl group from Me-Cbl to homocysteine (R-SH) in the methionine ($R-S-CH_3$) synthase enzymatic reaction is in the activation of the Co−C bond for bond breaking. The mechanism of formation of methionine from homocysteine has been discussed by Matthews[10] in terms of three possible pathways: (i) an S_N2 nucleophlic substitution, (ii) a reductive elimination reaction, and (iii) a methyl group transfer followed by an electron transfer, which was called a single-electron-transfer (SET) mechanism. Mechanisms (i) and (ii) can be viewed as having the same initial step if homocysteine thiolate ($R-S^-$) is the nucleophile, CH_3-Cbl the substrate, and $\{RS^{\bullet}\text{- -}CH_3\text{-Cbl(I)}^-\}$ the transition state, with $Cbl(I)^-$ as the leaving group. In this way a polar S_N2 mechanism can be viewed as having an inner-sphere ET through a methyl bridging group as an elementary step, followed by caged $RS^{\bullet} + {}^{\bullet}CH_3$ radical coupling to give methionine. As pointed out by Savéant,[29] in a valence bond sense this transition state should involve mixing of $\{RS^{\bullet}\text{- -}CH_3\text{-Cbl(I)}^-\}$ with other configurations, such as $\{RS^{\bullet}\text{- -}{}^-CH_3\text{-Cbl(III)}\}$, as a good multireference electronic structure calculation would show. In fact, our results indicate that the molecular orbital electronic configuration of this transition state needs to include such considerations.

Savéant[29] has also pointed out that, if this transition state is viewed as the result of an inner-sphere ET mechanism, one still needs to determine at what point ET occurs and at what point bond breaking and coupling occur. This is just the difference between mechanisms (i) and (ii) and mechanism (iii) discussed by Matthews.[10] In the methionine synthase enzymatic reaction, Zn^{2+} coordinates the homocysteine as a thiolate in the Hcy binding domain of the enzyme. In the S_N2 mechanism, this coordination should allow the energy of the frontier HOMO of the thiolate to approach the vacant LUMO of Me-Cbl, promoting the electron shift process. We propose that the interaction between the thiolate sulfur and the Me-Cbl should provide a large stabilization energy in the initial stage of the reaction so that the π^* bound state and the σ^* dissociative state move down and closer together, promoting the C−Co bond-breaking step.

The difference between the first two pathways and the SET mechanism (iii) is that, in the latter, the methyl group is transferred first, requiring homolytic bond breaking of Me-Cbl before the ET step, giving a histidine759 bound to Cbl(II) and a methionine radical anion bound to the Zn ion. Then the ET step occurs from the methionine radical anion to reduce base-on Cbl(II) to base-off $Cbl(I)^-$, with methionine formed in the process. In this SET mechanism, there must be an unknown protein configuration effect which activates the homolytic bond breaking for methyl transfer.

The reductive cleavage mechanism at electrodes for Me-Cbl in mixed DMF/alcohol solvent shows the involvement of the base-off reaction after radical anion formation. This result, along with the DFT calculations, which show a lower barrier for Co−C bond breaking for the base-off radical anion species, suggests that the transition state in the enzymatic mechanism should also involve such a base-off species. Some preliminary theoretical modeling of the S_N2 enzymatic mechanism for methionine synthase has been done using the single-reference DFT method.[62] Our results suggest that such modeling should be done with a higher order quantum mechanical calculation method.

Acknowledgment. This research was supported by NIH/NIGMS/SCORE grant GM08168 and NCSA grant CHE050065 for teragrid computer facilities. The authors thank J. R. Lombardi, B. Kräutler, J.-M. Savéant, and R. G. Finke for helpful discussions.

Supporting Information Available: Complete ref 20; simulations of cyclic voltammetry for a multistep mechanism (Scheme 3) as function of K_{23} and K_{35} (Figure S1); comparison of a multistep to a simple EC mechanism (Figure S2); CV curves for a quasi-reversible electrode EC process as a function of the rate constant of a subsequent chemical reaction (Figure S3); energy level plots from DFT calculations for methylcobalamin (model 1), its base-on and base-off one-electron-reduced forms, and its Co(I) form (Figure S4); and chemical preparation methods for alkylcobalamins. This material is available free of charge via the Internet at http://pubs.acs.org.

JA054479C

(62) Jensen, K. P.; Ryde, U. *J. Am. Chem. Soc.* **2003**, *125*, 13970.